Final Progress Report for Project Entitled:

Quantum Dot Tracers for Use in Engineered Geothermal Systems

DE-EE0002768

Peter Rose[1], Principal Investigator; Michael Bartl[2], Co-Investigator; Paul Reimus[3], Co-Investigator, Mark Williams[4], Co-Investigator; and Mike Mella[1]

[1]EGI, University of Utah
[2]Department of Chemistry, University of Utah
[3]Los Alamos National Laboratory
[4]Pacific Northwest National Laboratory

Executive Summary

The objective of this project was to develop and demonstrate a new class of tracers that offer great promise for use in characterizing fracture networks in EGS reservoirs. From laboratory synthesis and testing through numerical modeling and field demonstrations, we have demonstrated the amazing versatility and applicability of quantum dot tracers. This report summarizes the results of four years of research into the design, synthesis, and characterization of semiconductor nanocrystals (quantum dots) for use as geothermal tracers.

In Year 1, we modified a low-temperature, hydrophobic-solvent synthesis to one that rendered the quantum dots water-soluble through a ligand-exchange method. This approach resulted in very luminescent quantum dots, which, unfortunately, were not very resistant to oxidation under ambient conditions. Therefore, a method was adapted that involved covering the CdSe core with a thin shell of protective crystalline CdS—to create a core/shell quantum dot. This shell not only minimized oxidative effects but served to minimize surface defects of the CdSe core crystallite—thereby enhancing its fluorescence quantum yield. To further improve resistance to oxidation, a silica encapsulation approach was subsequently developed and tested. Following treatment under autoclave conditions that simulated a geothermal environment, the luminescence of the silica-coated quantum dots was enhanced—showing promise for an improved synthesis technique.

During Year 2, a major objective was to develop and demonstrate a method for increasing the diameters of quantum dots while preserving their luminescence. This would allow for the adjustment of an important parameter—the diffusion coefficient. The diameter was increased by increasing the thickness of the protective outer silica layer through a seeded sol-gel method. The luminescence was preserved by simultaneously increasing the number of individual core/shell quantum dots within each silica sphere. Subsequent thermal stability testing under conditions that simulated a geothermal environment revealed a three-fold enhancement of luminescence upon treatment at 300°C for 8 hours, a result that was foreshadowed by earlier thermal experiments during year 1. The silica surface was chemically activated during the treatment, however, initiating a gradual agglomeration of the silica-coated core/shell colloids. We then investigated several new silica precursor compounds in terms of the stability of the formed glass-like protection layer around the quantum dots with 3-mercaptopropyl trimethoxysilane (MPTS) showing the best performance. But even MPTS was incapable of inhibiting agglomeration under aggressive, high temperature conditions. We then realized that it would be necessary to coat the quantum dot tracers with a single layer of bi- or tri-functional molecules. One of the functionalities would be chosen to bind to the quantum dot surface, whereas the other functionality has a very low affinity for quantum dots but will render them water-soluble. Also during Year 2, we designed and initiated fabrication of a novel flow reactor that could be used to characterize the quantum dot tracers under realistic hydrothermal conditions. Since colloids are affected by gravitational forces, the reactor was configured for flow in either a vertical or horizontal direction. It was also designed to allow for simulating an injection/backflow test, which is common for EGS tracer testing. Finally, the Multran (LANL) numerical simulation code was modified to accommodate reversible tracer adsorption in anticipation of a field test of the quantum dot tracers.

In Year 3, we addressed the problem of long-term stability under room-temperature, oxidative conditions. This problem resulted from an inadequate ligand chemistry that has caused the colloidal nanoparticles to coalesce and precipitate from solution. New ligand chemistry was therefore designed to provide for long-term room-temperature stability under oxidative conditions. Upon adjusting a wide range of parameters, it was found that the quantum dots' luminescence is particularly sensitive to the pH and sodium citrate (ligand) concentrations. Of particular importance, it was discovered that extensive purification of CdSe/CdS quantum dots particles to remove excess monomer precursors resulted in highly monodisperse samples that were subsequently shown to be only slightly altered (blue-shifted) upon treatment to laboratory-geothermal conditions at 150°C. Several equally stable colors (different sizes) of CdSe/CdS core/shell quantum dots were synthesized and likewise shown to be stable at 150°C. Significant progress was also achieved during Year 3 in the synthesis of core-shell-shell structures that have a silica protective layer (CdSe/ZnS-SiO_2) by using a novel microemulsion synthesis technique. This technique created a denser silica shell and, importantly, the reactivity of the silica shell was strongly reduced, thus preventing uncontrolled crosslinking and increasing the quantum dot stability in solution. Quantum dots synthesized using this technique showed no loss in luminescence and only a slight shift in wavelength following autoclave treatment at 150°C. Also during Year 3, a tracer test was conducted in the Soda Lake geothermal reservoir using a conservative solute tracer in combination with a reversibly-adsorbing solute tracer. Since sufficient quantities of quantum dot tracers were not available, the solute tracers served as proxies for conservative and reversibly-adsorbing semiconductor nanocrystals. Numerical simulation models were developed at LANL and at PNNL and used to fit the data from the field experiments. Upon inversion of the data, it was possible to calculate the tracer-contacted fracture surface area—a first ever measurement of this very important parameter in a geothermal reservoir.

During Year 4, improved methods for the synthesis of CdSe/ZnS/SiO_2 core-shell-shell quantum dots were developed resulting in no loss of luminescence after treatment in an autoclave under simulated geothermal conditions at 250°C. Flow experiments using a solution of 'conservative' 2.6-nm CdSe/CdS/citrate quantum dot tracers flowing through a sand-filled column reactor showed a contrast with the performance of a conservative solute companion tracer. This contrasting behavior was modeled using the LANL semi-analytical code RELAP, which captured reasonably well the behavior of both the solute and colloidal tracers. We made significant progress in tuning synthesis parameters, resulting in an increase in yield by a factor of about 1000. We also investigated routes to scale up our quantum dot synthesis method from the current 50-milliliter-per-synthesis run (lab scale) to liter scale and, eventually, to hundreds-of-liters scale for field testing. We demonstrated a 10-fold increase in synthesis volume without loss of the high quality and stability of quantum dots.

Table of Contents for Phase I, Year 1

Project Objectives

Phase 1

The objective of this project is to develop and demonstrate a new class of tracers that offer great promise for use in characterizing fracture networks in EGS reservoirs. From laboratory synthesis and testing through numerical modeling and field demonstrations, we will demonstrate the amazing versatility and applicability of colloidal quantum dots as conservative (nonreactive) tracers. Through modifications of surface properties and diameters, they will then be transformed into reactive tracers that will sorb and diffuse in predictable ways with fracture surfaces and thereby be used to determine fracture surface areas.

Phase 1, Subtask 1: Design and synthesize first-generation nonsorbing quantum dot tracers (Bartl group)

Proposed Approach

At least three distinct quantum dot tracers that fluoresce in the visible (400-750 nm), one that fluoresces in the near IR (800-950 nm), and one that fluoresces at longer IR wavelengths (950-2000 nm) will be synthesized in sufficient quantity for subsequent testing. Four different compositions of colloidal nanocrystals (all with sizes varying from about 1 to 10 nm in diameter) will be used to cover the targeted emission wavelength range from 450 to 1500 nm: cadmium selenide (CdSe; 450-650 nm), cadmium telluride (CdTe; 600-750 nm) and lead sulfide and selenide (PbS and PbSe; 750-2000 nm).

Synthesis will be done using the low-temperature method that has recently been developed in the lab of one of the PIs (Bartl and Siy, 2009a; Bartl and Siy, 2009b). This method will enable us to fabricate quantum dots with narrow size distributions and therefore narrow emission bands of only several tens of nanometers. The quantum dot tracers will therefore possess sufficiently distinct emission spectra that they can be simultaneously measured by relatively simple and inexpensive spectroscopic techniques. In order to optimize the photoluminescence emission yield, all nanocrystals will be synthesized as so-called core-shell structures by surrounding them with a thin layer of cadmium sulfide (CdS).

Accomplishments

Second Quarter

Initial efforts focused on synthesizing CdSe-based quantum dots that are water-soluble and have tunable fluorescence in the visible. For this, a synthesis method was adapted from literature reports that results in CdSe quantum dots with citrate molecules attached to their surface, rendering them water-soluble. The synthesis conditions were varied to fabricate quantum dots with different sizes (3-5 nm in diameter), resulting in green, yellow and orange emission colors. Furthermore, so-called core-shell structures were synthesized by covering the CdSe quantum dots with a thin shell of crystalline CdS. This extra shell minimizes surface defects of the CdSe core crystallite and thereby enhances the fluorescence quantum yield. Current efforts focus on

optimizing these core-shell architectures to produce water-soluble quantum dots with fluorescence quantum yields approaching those of conventionally used organic dye tracers.

In parallel to CdSe-based quantum dot synthesis we have also began to fabricate PbS quantum dots. The advantage of PbS is an inherently smaller electronic band gap, which shifts electronic and optical properties of PbS quantum dots into the near infrared range. So far we have successfully fabricated fluorescent PbS quantum dots with emission bands centered between 900 and 1000 nm. A current limitation of PbS quantum dots, however, is that synthesis routes require very hydrophobic (oily) conditions and as a result the synthesized quantum dots are insoluble in aqueous media. A central focus of current and future research is therefore to extend the water-based synthesis route that we successfully applied for CdSe quantum dots to PbS quantum dots.

Third Quarter

In the previous quarter, we adapted a method from literature reports that desribed the synthesis of CdSe quantum dots with citrate molecules attached to their surface, rendering them water-soluble. Using this method we were able to fabricate CdSe quantum dots and CdSe/CdS core-shell quantum dot structures with different sizes (3-5 nm in diameter), resulting in green, yellow and orange emission colors. Unfortunately, we discovered that these quantum dots are prone to strong surface oxidation and are not stable over extended times in aqueous solutions. In detail, after a few days the quantum dot luminescence diminishes and the quantum dots precipitate and finally crash out of solution. We therefore decided to focus on our second approach for fabricating water-soluble quantum dots: namely by first fabricating high-quality hydrophobic quantum dots by our low-temperature method that enables up-scaled fabrication of highly luminescent and stable quantum dots. These quantum dots will then be converted into water-soluble and water/oxidation-stable quantum dots by surface ligand-exchange methods as described in the following section.

Fourth Quarter

This subtask is 100% complete.

Phase 1, Subtask 2: Design and synthesize highly-luminescent nonsorbing water-soluble quantum tracers (Bartl group)

Approach

The surface chemistry of highly-luminescent core-shell quantum dots will be tuned to give optimized interaction with the sensing/tracing environment. We will explore two strategies to achieve this goal:

1) Fabrication of initially hydrophobic quantum dots using our low-temperature method and rendering them water-soluble in a second step by surface-ligand exchange (amine, carboxy, or thiol-functionalized ligands).
2) Modification of our low-temperature synthesis route for the direct synthesis of hydrophilic nanocrystals with water-soluble surface ligands (citrate or hydroxyl-functionalized ligands).

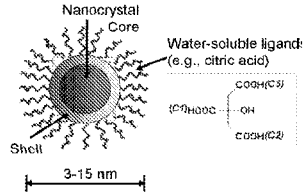

Figure 1. *Schematic depiction of a water-soluble core-shell nanocrystal quantum dot tracer.*

While the latter requires less fabrication steps, the first strategy is better established and therefore will allow faster product availability with better control of size and properties of the synthesized quantum dot tracers. Initially, we will explore both strategies and will then decide – after preliminary feasibility/applicability studies – which method is best suited for the proposed activities. A schematic of the structure of water-soluble quantum tracers is shown in Figure 1.

Accomplishments

Second Quarter

Initial studies showed that CdSe and PbS-based quantum dots can be made water-soluble and display tunable fluorescence emission in the visible and near IR range, including the important 800 to 1000 nm wavelength range. These initial results are very encouraging and studies in the last funding period focused on up-scaling quantum dot production. Up-scaling of quantum dot production will be of great importance for field testing in an injection/backflow test in an EGS wellbore. However, up-scaling of conventional synthesis methods is generally a problem due to the high reaction temperatures (230-350 °C), which lead to the formation of temperature gradients in large reaction volumes. In addition, due to the fast nucleation and growth kinetics at high reaction temperatures injection of precursors has to occur very rapidly to avoid products with large unwanted size polydispersity.

We have recently developed a low-temperature (50-130 °C) synthesis route for the fabrication of high-quality colloidal nanocrystals. We recently were able to demonstrate first results, showing that the lowered synthesis temperatures allow up-scaling of CdSe quantum dot production. Up-scaling is pursued in two steps: 1) Increasing the concentration of produced quantum dots per reaction volume and 2) increasing the reaction volume per run. So far we focused on step 1 and were able to increase the concentration of quantum dots by a factor of 1000. This was accomplished by optimizing the ratio of quantum precursor components to surface-stabilizing ligands. Importantly, up-scaling did not lower the quality (structural and optical properties) of the synthesized CdSe quantum dots. The next steps will be to 1) continue optimizing the reaction

parameters to further increase the production and 2) build a synthesis set-up that will enable increase of the reaction volume from currently 10-20 milliliters to several liters.

We continued to optimize up-scaling of our low-temperature synthesis procedure for high-quality semiconductor nanocrystals ("quantum dots"). Up-scaling is pursued in two steps: 1) Increasing the concentration of produced quantum dots per reaction volume and 2) increasing the reaction volume per run. The ultimate goal is to reach synthesis batch levels high enough to directly use quantum dots as luminescent tracers for field testing in an injection/backflow test in an EGS wellbore.

In the previous funding period we made significant progress in tuning synthesis parameters, resulting in an increase in yield-per-synthesis-run by a factor of about 1000. Since then we focused on optimizing the optical properties of the quantum dots synthesized at such high yields. We made significant progress and achieved quantum dot qualities in terms of optical and structural properties equal to those synthesized at low concentrations and/or high temperatures. This is also evidenced in the narrow optical absorption and emission peak features (with full-width-at-half-maximum values as low as 30 nm) shown in Figure 2.

The second main aspect of our current research is aimed towards up-scaling the overall reaction volume. For this, we built a new quantum dot synthesis set-up that will allow increase of the per-batch reaction volume by a factor of up to 200 (from the current 20 mL to about 4 L). Figure 3 shows a photograph of the set-up and we are currently in the finishing stages of linking the various synthesis apparatus components and starting with quantum dot synthesis runs at these high reaction volumes.

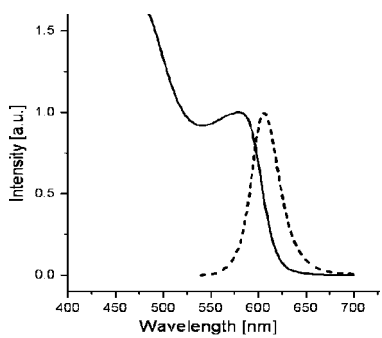

Figure 2. *UV-vis absorption (full line) and photoluminescence emission (dotted line) spectra of CdSe nanocrystal quantum dots produced at low reaction temperatures (130 C) and high yield (1000 fold increase).*

Figure 3. Photograph of high-reaction-volume synthesis set-up for up-scaled quantum dot production.

Third Quarter

As described in detail in our last quarterly report, our initial work was focused on up-scaling quantum dot synthesis to reach levels necessary for field testing in an injection/backflow test in an EGS wellbore. Meanwhile, we are able to produce quantum dots with excellent optical properties on gram scales per synthesis run. In parallel with these up-scaling efforts we initiated studies to convert these as-synthesized oil-soluble quantum dots into water-soluble products by replacing their original hydrophobic surface coverage with a hydrophilic one. A schematic of our approach is shown below.

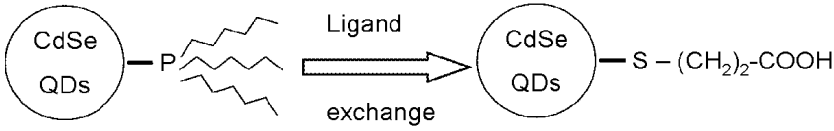

Figure 4. *Schematic reaction pathway for converting as-synthesized hydrophobic CdSe quantum dots (QDs) into water-soluble quantum dots.*

In this approach, termed "ligand exchange", we exchange the hydrophobic ligands (alkylphosphine based) with hydrophilic ligands such as 3-mercaptoproprionic acid. This is done by vigorously mixing an as-synthesized quantum dot solution in chloroform as solvent with an aqueous solution of 3-mercaptoproprionic acid. During the mixing, the ligand exchange reaction takes places, resulting in water-soluble quantum dots. While this process is very simple and fast, unfortunately, we also found that the luminescence efficiency of the quantum dots is reduced after the exchange reaction. This is most likely due to surface defects that were created during the ligand exchange. In order to overcome this problem, we are currently developing methods compatible with our low-temperature large-scale synthesis approach to protect the CdSe surface by first covering it with a thin layer of CdS or ZnS. Such core-shell structures have the advantage of minimizing surface defects of the CdSe core crystallite and thereby enhance the fluorescence quantum yield.

Fourth Quarter

A central focus of activities in this funding period was to study in detail the surface chemistry of our water-soluble quantum dots following the ligand exchange (see previous quarters). The goal was to understand the reactions occurring at the quantum dot surface that lead to the unwanted reduction in the photoluminescence emission efficiency and develop synthetic methods to overcome this problem. Using a combination of various optical spectroscopy tools including UV-vis absorption, photoluminescence emission, FTIR and Raman we were able to reconstruct the surface reactions. We performed these studies under different environmental conditions (room light, UV light, dark; under oxygen or nitrogen atmosphere). The results revealed that after ligand exchange the CdSe units at the surface of the quantum dots are prone to oxidation. This forms an initially thin layer of CdO. While a thin layer of CdO (2 to 3 atomic layers) is beneficial and enhances their emission efficiency, unfortunately, the oxidation continuous and slowly transforms the CdSe quantum dots into CdO particles, which coagulate and precipitate out of solution. In addition, this oxidation process is sped up under visible and UV light illumination (see Figure 5 below). In response to these results we decided to switch from pure CdSe quantum dots to core-shell CdSe/CdS quantum dots. As mentioned above, while such core-shell structures should have the benefit to increase the emission efficiency, we also anticipate that the thin CdS surface layer will provide a barrier preventing unwanted oxidation of the CdSe core quantum dot. First use of these core-shell quantum dot structures is described in Phase 1, Subtask 4.

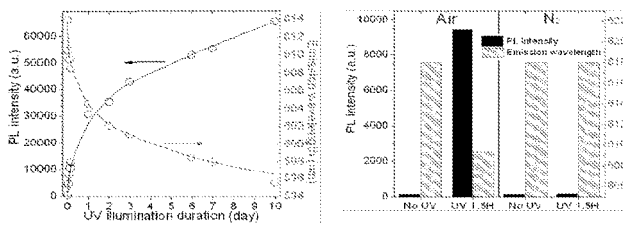

Figure 5. *Effect of UV illumination (left) and air/nitrogen exposure (right) on the surface oxidation and optical properties of CdSe quantum dots.*

This subtask is 100% complete.

Phase 1, Subtask 3: Develop a numerical model to predict fracture surface area adjacent to an EGS wellbore based upon the behavior of nonsorbing quantum dot tracers with varying diffusivities

Approach

A numerical model was developed to estimate both surface area and uncertainty in surface area from differences in single-well breakthrough curves of tracers with contrasting diffusivities.

Accomplishments

Third Quarter

An existing numerical model capable of simulating single-well tracer tests was exercised using diffusivities expected for quantum dot tracers, and the model provided stable solutions over a relatively wide range of assumed fracture apertures and matrix porosities, indicating that it should be suitable for estimation of fracture surface area from single-well tests over a wide range of potential EGS reservoir conditions.

Fourth Quarter

The numerical model described above (third quarter) was successfully modified to simulate heat transport (in addition to mass transport) in either single-well or cross-hole tracer test configurations. This capability was added to allow either diffusion coefficients or sorption parameters to be specified as a function of temperature, which may vary in EGS reservoirs by as much as 200C. Such variations could cause as much as five- to six-fold differences in diffusion coefficients of the same tracer in hot and cold parts of the reservoir and potentially similar differences in sorption parameters in different parts of the reservoir. The heat transfer features of the model were tested for several known simple cases and found to provide accurate solutions, although the time step size had to be reduced significantly relative to mass transport problems in the same geometry because of the much greater rate of thermal diffusivity relative to mass diffusivity. The capability to account for the temperature dependence of diffusion coefficients and sorption parameters will be added to the model in upcoming quarters (right now only temperatures are simulated and tracer properties are not directly linked to temperature, although this should be a relatively straightforward enhancement).

Phase 1, Subtask 4: Fabricate temperature and corrosion-stable nonsorbing quantum dot tracers (Bartl group)

Approach

Water-soluble core-shell nanocrystals will be immersed in a solution containing amino or thiol-functionalized alkoxysilanes, which serve as the molecular precursor for the glassy silica layer (Rogach et al, 2000). Formation of a continuous silica film is then induced by chemically cross-linking the alkoxysilane precursor and the thickness of the protective glassy layer is controlled

by the length of reaction. Initially, we will aim for a layer thickness of about 2-5 nm, resulting in total nanocrystal sizes between 5 and 25 nm. While this should be sufficient to protect the enclosed nanoparticles from corrosion and temperature, fine-tuning of the layer-thickness will be done in response in first high-temperature studies, simulating EGS conditions.

Besides temperature and corrosion-stability, another advantage of silica-coated quantum dot tracers is that the overall size of the tracer can be controlled without affecting the intrinsic tracer properties (e.g., emission color). We will make use of this by applying a layer-by-layer approach to gradually and predictably increase the overall size of the quantum tracers. A schematic is depicted in Figure 6. By changing the diameters, quantum dot tracers having contrasting diffusivities can be synthesized. These diffusivities can then be incorporated into a model that could serve to predict fracture surface area adjacent to an EGS well based upon diffusive-tracer data from an injection/backflow experiment.

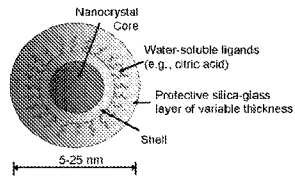

Figure 6. *Schematic depiction of a silica-glass coated core-shell quantum dot tracer with adjustable overall thickness.*

Accomplishments

Third Quarter

We developed a sol-gel chemistry-based method termed "silica encapsulation" (see schematic in Figure 7 below) to form a stable (and light-transparent) silica glass layer around the quantum dots.

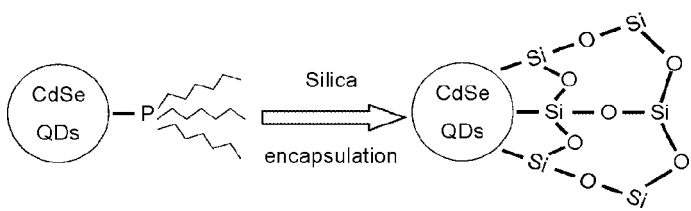

Figure 7. *Schematic reaction pathways for encapsulating as-synthesized hydrophobic or ligand-exchanged hydrophilic CdSe quantum dots (QDs) into a heat and corrosion-stable silica glass layer of adjustable thickness.*

This method not only renders quantum dots water-soluble and heat- and corrosion-stable, but it also retains the high luminescent yield of the original quantum dots by reducing their surface defects by covering them with a new silica surface layer. This solution-based process is rather simple and fast. As-synthesized quantum dots in chloroform (Figure 8; left vial, bottom layer) are combined with an aqueous solution of a silica precursor (tetraethyl orthosilicate) and potassium hydroxide (top layer). After reaction, the quantum dots transfer from the hydrophobic chloroform to the hydrophilic water phase, forming a stable solution (Figure 8; right vial).

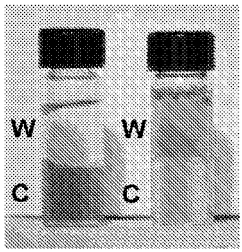

Figure 8. *Distribution of quantum dots in a chloroform(C)/water(W) two-phase system before (left) and after (right) the silica encapsulation*

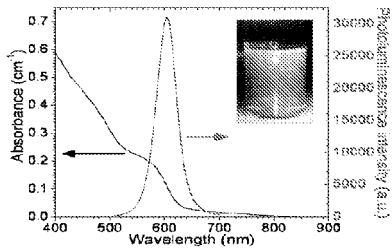

Figure 9. *Optical absorption (black) and photo-luminescence emission (red) spectra of water-soluble silica-encapsulated quantum dots.* ***Inset:*** *Emission photograph of quantum dots excited by a broadband UV lamp.*

Importantly, using the silica encapsulation process the quantum dots fully retain their excellent optical properties and display efficient luminescence emission efficiency at visible wavelengths as shown in Figure 9. The first prototypes of silica encapsulated quantum dots are currently used for studying their behavior in simple wellbore simulation environments (high temperatures and pressures; dissolved mineral solutions etc).

Another beneficial effect of the encapsulation process is that by varying the thickness of the silica shell the actual overall size of the "composite nanoparticles" can be varied without changing the emission color of the interior quantum dot. This property will be of great value in the later part of our proposed project in which the difference in size will be used to explore EGS wellbore fractures and surface areas.

Fourth Quarter

Unfortunately, we discovered that the silica-encapsulated CdSe quantum dots described in the last quarter report lose their initially bright luminescence when kept in air and room light conditions. As discussed in the 4th quarter report for Phase 1, Subtask 2, we investigated this phenomenon and found that core-only CdSe quantum dots undergo a surface oxidation process in aqueous solutions. This process not only reduces the CdSe quantum dot core size (since part of the quantum dot is oxidized to CdO), but as a result also irreversibly changes their optical properties: blue-shift of the emission color and reduction of emission efficiency over time. To overcome this problem, we applied our silica encapsulation method to core-shell CdSe/CdS quantum dots (synthesized using our low-temperature route described in detail above). Results are shown in Figure 10 below and clearly demonstrate that this approach is much more effective. While silica-encapsulated core-only CdSe quantum dots blue-shifted and lost almost all of their emission intensity (red spectrum), the core-shell analogs are still brightly luminescence (black spectrum.

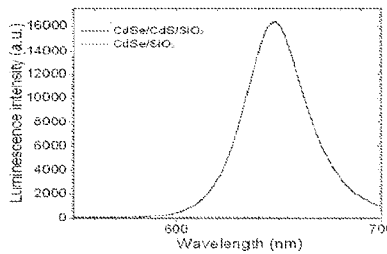

Figure 10. *Photoluminescence emission spectra of water-soluble silica-encapsulated core only CdSe (red) and core-shell CdSe/CdS quantum dots (black).*

This subtask is 80% complete.

Phase 1, Subtask 5: Determine the thermal stabilities of the nonsorbing quantum dot tracers under conditions that simulate an EGS reservoir (EGI group)

Approach

Using batch autoclave reactors, each tracer will be screened for thermal stability under conditions of temperature, pressure and chemistry that simulate a hydrothermal environment. For each tracer that survives the screening, its thermal decay kinetics will be determined using previously established methods (Rose et al, 2001).

Accomplishments

Third Quarter

Exposing the quantum dot tracers to simulated geothermal conditions may result in structural changes, which would in turn affect the optical properties of the nanoparticles. An emission spectrum (excitation at 400 nm) of a sample of quantum dots is shown in Figure 11.

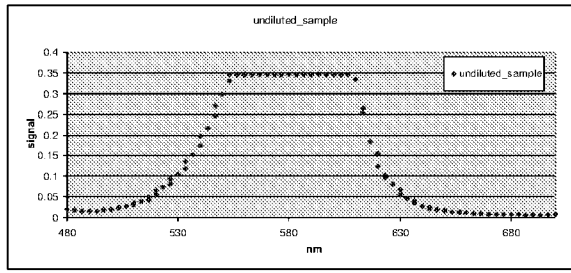

Figure 11. Emission spectrum of 5μM quantum dot sample.

The signal was very strong and saturated the detector, but the spectrum showed a peak centered near 580 nm.

The solution was diluted and placed in an autoclave reactor and heated to 250°C for 2.5 days. Emission spectra were measured for each of the samples, labeled #1 through #4, along with two control samples that had been maintained at room temperature, labeled C1 and C2. The emission spectrums are seen below as Figure 12.

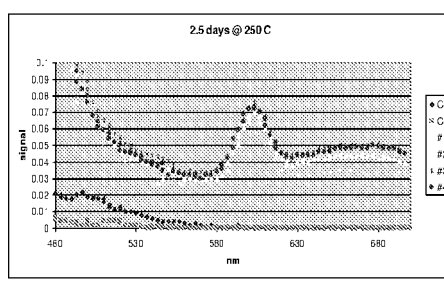

Figure 12. Emission spectrum of quantum dots subjected to heat treatment.

In this plot the heated samples exhibited a fluorescence peak centered near 600nm. In contrast, the control samples show no fluorescence. Evidently, the heating process appears to have enhanced the fluorescence of the quantum dots in this sample solution.

Fourth Quarter

A sample of first generation quantum dots was diluted 1:10, placed in quartz ampules and baked in autoclaves at EGI for a period of 5 days at 250°C. Emission spectra with an excitation wavelength of 400 nm were collected for the 3 baked samples, labeled #1, #2 and #3 in Figure

13. These are compared with an uncooked solution labeled 8/17/2010 1:10. The baked samples show that they have a peak in the region of the emission peak but shifted by about 15-20 nm and are larger magnitude signals. This is consistent with earlier results that showed a similar shift in emission upon heating. In a like manner the signal strength was once again shown to be higher. The increase in fluorescence suggested a fundamental change in the structure of the quantum dots during the heating process. Oxidation of the outside layer of the quantum dots resulted in both increase in fluorescence and a shift in the wavelength of emitted light as the size of the CdSe quantum dot changed. When the samples were first collected, a measurement was made for a dilution of 1:10 and this sample is on the plot below labeled as 8/2/2010 1:10. Comparison with the control sample measured 15 days later shows a marked reduction in fluorescence intensity with time. It would appear that the quantum dot tracers do not maintain stability over time if left in the dark. Modifications to the synthesis as described in subtasks 2 and 4 will likely make large differences in the thermal stabilities of the quantum dot tracers that will be tested in subsequent stability experiments.

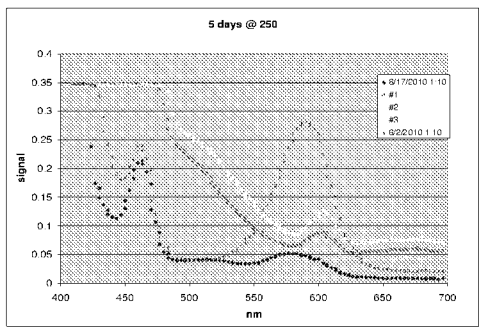

Figure 13. Emission spectrum of quantum dots subjected to heat treatment and change with time.

Phase 1, Subtask 6: Using liquid chromatography, characterize the flow properties of the nonsorbing quantum dot tracers under ambient conditions

Approach

At this point, a family of quantum dot tracers will have been synthesized with each member possessing a distinct diameter and, therefore, a distinct emission fluorescence. The diffusive behavior of the quantum dot tracers will be tested by size-exclusion chromatography (SEC) with fluorescence detection within our laboratory. These studies will provide a pore/fracture-dependent scaling factor of the retention time, which will be of enormous value in interpreting results from EGS investigations. The numerical model developed under Subtask 4 will be used to help interpret these test results.

Phase 1, Subtask 7: Go/No-Go Decision

A Go/No-Go decision was built into the project such that if, at the end of the first year, thermally stable and corrosion-resistant nonsorbing quantum dot tracers had not been fabricated and demonstrated that meet the requirements of the tasks outlined above, then the project would be terminated. The conditions of the Go/No-Go decision were met and the project continued.

Figure 14 below is a Gantt chart showing the expected start and completion dates of each of the subtasks throughout the three years of the project.

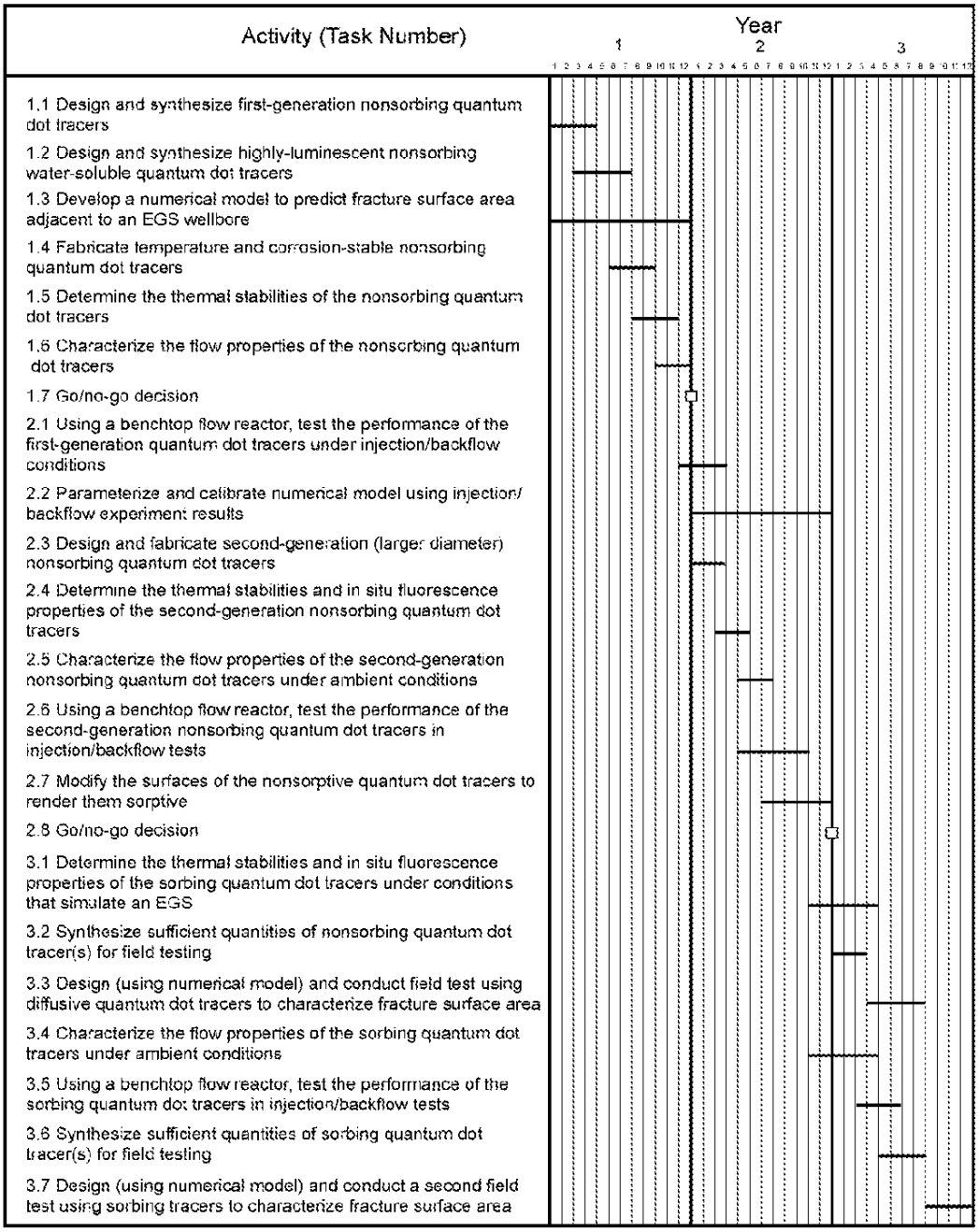

Figure 14. Gantt chart summarizing the Project Management Plan.

Phase II, Year 2

Progress Report for Year Ending September 30, 2012:

Quantum Dot Tracers for Use in Engineered Geothermal Systems

DE-EE0002768

Peter Rose[1], Principal Investigator; Michael Bartl[2], Co-Investigator; Paul Reimus[3], Co-Investigator, Mike Mella[1], Kevin Leecaster[1], Bridget Ayling[1], Eric Brauser[1], Vince Vermeil[4], Mark Williams[4], and Susan Petty[5]

[1]EGI, University of Utah
[2]Department of Chemistry, University of Utah
[3]Los Alamos National Laboratory, Los Alamos
[4]Pacific Northwest National Laboratory
[5]AltaRock Energy Corporation

Table of Contents for Phase II, Year 2

Project Objectives

Phase 2

The objective of this project is to develop and demonstrate a new class of tracers that offer great promise for use in characterizing fracture networks in EGS reservoirs. From laboratory synthesis and testing through numerical modeling and field demonstrations, we will demonstrate the amazing versatility and applicability of colloidal quantum dots as conservative (nonreactive) tracers. Through modifications of surface properties and diameters, they will then be transformed into reactive tracers that will sorb and diffuse in predictable ways with fracture surfaces and thereby be used to determine fracture surface areas.

Phase 2, Subtask 2.1: Test the performance of the first-generation nonsorbing quantum dot tracers under conditions that simulate an injection/backflow test in an EGS wellbore

Proposed Approach

The flow reactor will be adapted to simulate a newly sheared fracture, complete with a porous, altered-vein mineral. An injection/backflow experiment will be conducted by injecting a solution of quantum dot tracers, followed by a shut-in phase, followed by a production phase—all at elevated temperature and pressure. The numerical injection/backflow model (Task 1.3) will be used to help design and interpret the experiment, and data from the experiment will in turn be used to calibrate and parameterize the model.

Accomplishments

First Quarter

LANL has completed the refabrication of a flow-through packed reactor, with successful initial tests at pressures and temperatures of 1500 psi and 250°C, respectively. Tracer experiments will start in the next few weeks. This reactor is designed to simulate either interwell or injection-backflow tracer tests. A similar reactor is being designed for deployment at EGI.

Second Quarter

One flow-through experiment was conducted at LANL at 1500 psi and 225 °C using 1,5-naphthalene disulphonate (NDS), bromide, and lithium as tracers. The reactor was packed with crushed rock from the former Fenton Hill (NM) EGS site, and a synthetic brine was used as the working fluid. The 1,5-NDS breakthrough curve indicated complete recovery of this tracer (within experimental error) with typical tracer dispersion behavior in the column. The lithium and bromide breakthrough curves were not yet available (awaiting chemical analysis) as of this writing. The experiment was terminated earlier than planned because a filter in the outlet line plugged, causing a pressure burst disc to pop when the experiment was unattended. It is unknown how much of the lithium was recovered before the premature termination of the experiment. Experimental modifications have been made to avoid this problem in the future.

Fourth Quarter

This quarter we were able to sponsor a graduate student from Stanford, Morgan Ames, with an internship. He collaborated with us on this research by helping to perform flow experiments with nanoparticles. We obtained 20 nm carboxylated fluorescent polystyrene and 20 nm carboxylated silica beads from commercial sources (Invitrogen & Active Motif). Because of the higher cost & lower detectability of the silica beads, we chose to test our procedures by first working with the polystyrene beads.

Because the nanoparticles have a high density of carboxyl groups they can agglomerate in low pH or high ionic strength solutions. In an attempt to obtain a low ionic strength solution that would not be significantly affected by the porous media, we created our base solution by eluting 30 ppm NaCl through the Ottawa sand. A portion of this was spiked with the nanoparticles and the conservative tracer 1,5 NDS. Two experiments at 25° C were performed attempting to measure the nanoparticle transport through the medium fraction Ottawa sand column that was previously used to test safranin T retardation. In the first experiment we didn't detect any nanoparticle breakthrough, but after the experiment it was determined that the solution pH was lower than expected (3.3) after the tracer addition to the base solution. This could have caused agglomeration of the particles such that the full concentration was not able to be pumped to the column and/or the higher proton concentration might have increased the quantity of positively charged sites on the quartz enough to have caused the beads to pass through the porous media. After more than 5 hours of flow, we disconnected the column and reconnected it so that we could backflush the column and monitor for nanoparticle fluorescence, but there was no clear evidence of the beads.

We repeated the experiment under the same conditions, but at a solution pH of 6.9 and while this time the nanoparticles did show up in the effluent the breakthrough curve doesn't clearly indicate that the beads did behaved conservatively in the porous media (see Figure 1). The fluorescence response of the effluent increased during the step injection up until 250 mL had been eluted and then started to decrease despite the step input continuing for twice that long. The microspheres appear to be retarded relative to the naphthalene-sulfonate tracer, but when the fluorescence data are normalized based upon the maximum concentrations it appears that they behaved conservatively during the flush step. We intend to repeat this test on the same media at a higher pH and with the silica particles.

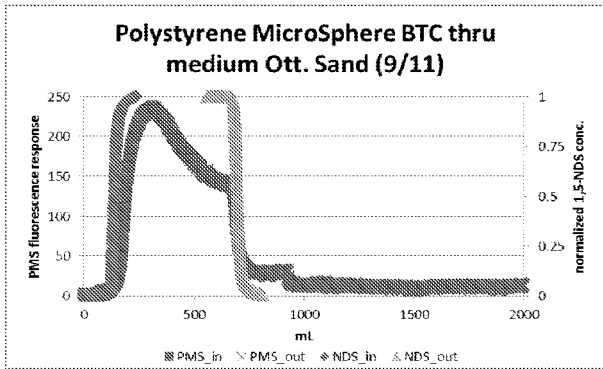

Figure 1. Response of fluorescent polystyrene nanoparticles and 1,5-naphthalene disulfonate tracer through the Ottawa sand column at ambient temperature and pH 6.9.

Phase 2, Subtask 2.1: Parameterize and calibrate numerical model using injection/backflow experimental results

Approach

The numerical model developed under Task 1.3 will be calibrated against the results of the flow reactor experiments of Task 2.1 above. Emphasis will be placed on verifying and parameterizing the target transport characteristics of the quantum dot tracers, especially their effective diffusivities relative to solute tracers and their nonsorbing behavior. It is important to note that any apparent sorption of the quantum dot tracers will not render them unusable for surface area estimation. Rates and capacities of sorption are proportional to surface area, so sorptive interactions can also be exploited to estimate surface area. If completely nonsorptive behavior of the quantum dot tracers proves elusive, the numerical model will be adapted to use sorptive interactions (or combined diffusive and sorptive behavior) to estimate surface area, and the necessary sorption rates and capacities will be estimated from the flow reactor data set (see also Task 2.8).

Accomplishments

First Quarter

The 2-D numerical code, MULTRAN (MULticomponent mass TRANsport) was modified to simulate simultaneous heat and mass transfer in either single-well or cross-hole tracer test configurations (it formerly solved only mass transfer in isothermal systems). The modifications include the capabilities to specify thermal decay of tracers and to account for temperature dependence of diffusion coefficients. Temperature dependence of cation exchange equilibrium

constants will be incorporated into the code in the next quarter. Also, the computational speed of the code will be improved by allowing larger time steps for mass transfer calculations than for heat transfer calculations. The latter require much smaller time steps because thermal diffusivity is much faster than mass diffusivity. Also, the mass calculations are much more expensive per time step because they involve as many sets of equations as there are components and the equations are more complex than for heat transfer because interactions between components must be accounted for. The code successfully ran several test cases.

Fourth Quarter

Paul Reimus (LANL):

The MULTRAN code was modified to include the capability to simulate a tracer that sorbs and desorbs according to a simple retardation process rather than by cation exchange. This capability will hopefully be applicable to both reactive quantum dot tracers and fluorescent dye tracers that have no net charge (or do not sorb by cation exchange). Also, test cases are being run to ensure that MULTRAN works properly for injection-backflow tests in a laboratory column reactor. The injection-backflow simulations that have historically been run in MULTRAN have used radial coordinates to simulate single-well field tests, but the laboratory experiments will require Cartesian coordinates to be fully accurate. Results of this testing are preliminary and will be discussed more next quarter.

Mark Williams and Vince Vermeul (PNNL):

The approach for developing a site-specific numerical model using ToughReact for single-well injection/backflow tracer tests at the Soda Lake site will initially require developing and simulating the existing interwell tracer test data sets conducted at the site (which included conservative and sorbing tracers). The interwell numerical model will be used to estimate site parameters from these tracer tests. The grid design for the simulations of the interwell tests may be different than needed for the single well tests. Numerical simulations using the field parameters from the interwell tracer test fitting process will then be developed for use in designing and the interpretation of single-well injection/backflow tests with sorbing, diffusing, and thermally degrading tracers. This single-well injection/backflow test simulations will be used to investigate test efficacy for determining insitu field-scale fracture properties based on operational parameters of the test (e.g. volumes, rates, duration) and investigating breakthrough curve responses from ranges of tracer properties measured in the laboratory.

Phase 2, Subtask 2.3: Design and fabricate second-generation (larger diameter) nonsorbing quantum dot tracers

Approach

At this point, first-generation quantum dot tracers will have been synthesized and characterized that possess small differences in diameter and, therefore, small contrasts in diffusivity. In this task, we will develop and demonstrate size-discriminating quantum dot tracer systems that possess much larger diameters. The strategy is to incorporate highly-luminescent core-shell quantum dots with distinct emission colors into a range of nano to 0.1-micrometer-sized glass

spheres. For example, blue, green, red, NIR emitting quantum tots will be selectively incorporated into glass spheres with overall diameters of 10, 25, 50 and 100 nm, respectively (Figure 2). Fabrication of such glass spheres will be done by sol-gel colloidal synthesis methods. One of the PIs (Bartl) has extensive experience in sol-gel fabrication (Cha et al, 2003; Bartl, 2002; Bartl et al, 2005; Galusha et al, 2008) and we will use his group's expertise to develop high-quality size-discriminating quantum dot tracers.

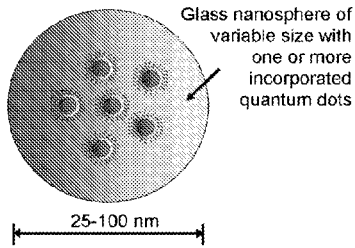

Figure 2. Cartoon of nanosphere showing the enhancement of fluorescence achieved by increased loading.

In short, core-shell quantum dots with a thin layer of silica on their surface (see Task 1.4) will be immersed in a solution containing molecular silica-glass precursors. The reaction conditions will be adjusted so that the silica-coated nanocrystals will act as seed colloids for controlled condensation of silica-glass precursors on their surface, resulting over time in the formation of spherical objects with adjustable sizes (depending on time of reaction). Since spheres differing in sizes over an order of magnitude will have distinctly different diffusive properties, their relative retention times will contain valuable information about fracture size, morphologies, surface area and spacing. Due to the unique electronic and optical properties of nanocrystal quantum dots, information of relative retention of all sphere sizes can be interrogated by simultaneously exciting all four emission colors by a single-wavelength source!

Whereas the silica coatings will increase the diameters of the quantum dots, they will also have the adverse effect of increasing particle density. We will explore within this task the use of organic polymeric compounds to "dilute" the silica as much as possible in order to create quantum dot tracers with densities closer to that of water, thereby rendering them more effective as diffusive tracers.

Accomplishments

First Quarter

In year 1 of the research activities we focused on developing robust composite tracers with a semiconductor CdSe quantum dot core (as the tunable light emission source) and a glass-like silica-based shell to encapsulate and protect the quantum dot from the potential harsh conditions

in geothermal wells. We developed a sol-gel silica formation method that is compatible with the chemistry of the CdSe quantum dots; i.e., with this method we do not significantly alter/modify the excellent luminescent properties of the quantum dots while at the same time rendering them water-soluble by coating with a thin silica layer. In subsequent longer-term studies, however, we found that, unfortunately, silica-coated CdSe quantum dots are prone to (photo-)oxidation when stored in aqueous media. This effect could largely be suppressed by synthesizing core-shell quantum dots. In these quantum dots the CdSe core is protected by a thin semiconducting shell of CdS or ZnS before over-coating with the silica layer. Initial studies showed that this method helps to stabilize the quantum dots and leads to longer and better emission properties (as described in the last quarterly report 1). Since then we studied and optimized this approach in great detail, focusing on the effectiveness of quantum dot stabilization and their behavior/robustness under high pressure and temperature conditions.

One of the important factors in the coating process of CdSe/CdS or CdSe/ZnS core-shell quantum dots with a uniform silica layer is the reaction time with the silica precursors (tetraethyl orthosilicate, TEOS) and the reaction composition. On the one hand, the reaction time needs to be long enough to sufficiently coat the quantum dots with silica and thereby making them water-soluble; on the other hand, if the time of reaction is too long, the silica-coated quantum dots themselves may react and form unwanted large interconnected clusters (unwanted, because these clusters are not stable in solution and precipitate). Since during the coating process the quantum dots transfer from the chloroform phase into the aqueous phase (see also previous report), we can monitor the coating process/efficiency simply by UV-vis absorption spectroscopy. Here, the UV-vis absorbance at the quantum dot exciton peak maximum is directly proportional to their concentration in solution (Beer-Lambert's law).

Some of the most important results of the broad optimization studies are shown in Figure 3 in which we have plotted the absorbance at the exciton peak maximum (~ 626 nm wavelength position) for different silica (TEOS) coating reaction times. For short TEOS reaction times (< 5 minutes) the amount of quantum dots transferred into water was very low. This amount increased strongly with TEOS reaction time and reaches a maximum after 15 minutes. Beyond this time, the quantity of quantum dots transferred into water decreases quickly and reaches a plateau after 60 minutes of TEOS reaction time. The small number of quantum dots transferred into water for low TEOS reaction time probably arises from a lack of TEOS linked to the quantum dot surface due to the low concentration of both quantum dots and TEOS in chloroform. On the other hand, beyond 15 minutes of TEOS reaction time the silica-coated quantum dots formed clusters, which precipitate out of solution and thus do not absorb, explaining the UV-vis absorbance decrease. Furthermore, it should be noted that the quantum dots were dissolved with twice the amount of water than chloroform; therefore, the fact that the UV-vis absorbance at the exciton position for quantum dots in water is half that of quantum dots in chloroform demonstrates that the transfer yield (i.e. ratio between amount of quantum dots in chloroform and in water) is 100% for a TEOS reaction time of 15 minutes.

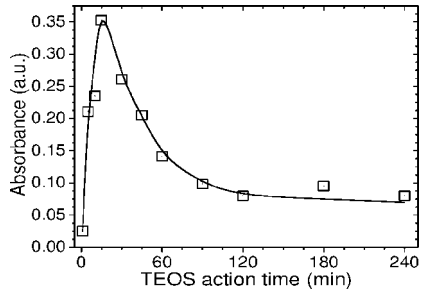

Figure 3. UV-vis absorbance at the exciton peak position (~ 626 nm) of quantum dots transferred into water as a function of TEOS reaction time.

Second Quarter

The research activities of this quarter were aimed toward the synthesis of first large-diameter quantum dot tracers (second generation nonsorbing quantum dot tracers). As outlined in the original proposal our approach was to use silica coated quantum dots as seed particles immersed in a solution of silica sol-gel precursor molecules. The deposition of additional silica around the quantum dot seeds was then induced by base-catalyzed hydrolysis and condensation reactions. The amount of additional silica deposition is a function of concentration of silica precursor and the time of reaction. First successful experiments were performed and yielded large silica spheres with tens of nanometer diameters and incorporation of several different quantum dots. A transmission electron microscopy image of one of the synthesized large silica spheres with incorporated quantum dots is shown in Figure 4.

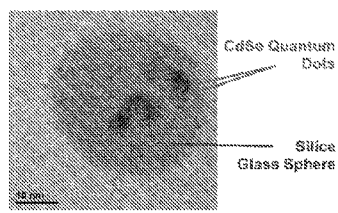

Figure 4. Transmission electron microscopy image of a large silica glass sphere with several incorporated CdSe quantum dots fabricated by our seeded sol-gel method.

Phase 2. Subtask 2.4: Determine the thermal stabilities and in situ fluorescence properties of the second-generation nonsorbing quantum dot tracers under conditions that simulate an EGS reservoir

Approach

Using batch autoclave reactors, each tracer will be screened for thermal stability under conditions of temperature, pressure and chemistry that simulate a hydrothermal environment. For each tracer that survives the screening, its thermal decay kinetics will be determined using previously established methods. Likewise, the in situ fluorescence of each tracer at high temperature will be determined.

Accomplishments

First Quarter

We initiated tests of the stability of silica-coated core-shell CdSe/ZnS quantum dots in water by hydrothermally treating them in a stainless steel autoclave at a temperature of 300 °C and a pressure of 40 MPa for 8 hours (see Figure 5). We choose such harsh conditions (higher temperatures and pressures than planned in initial in-lab and field testing) to speed up possible decay kinetics. The most important result is that even after such harsh treatment the silica-quantum dot composite tracers retained their emission ability. In fact, we found that *the emission efficiency more than tripled* (a phenomenon that is currently under investigation with the goal to take advantage of it in the future by proper quantum dot pre-treatment). We also found a strong blue-shift of the peak position from 635 nm to 510 nm, which, most likely, can be assigned to a strong CdSe cores size reduction, probably due to an oxidation process induced by the pressurized hot water. In current work we address this partial oxidation under the high pressure and temperature conditions and seek for additional ways to further stabilize the CdSe quantum dot cores. Hand in hand with these stabilization studies we have also begun to uniformly increase the silica coating thickness without causing clustering of multiple particles. These studies will be of great help for fabricating the second-generation non-sorbing quantum dot tracers with adjustable (larger) diameters.

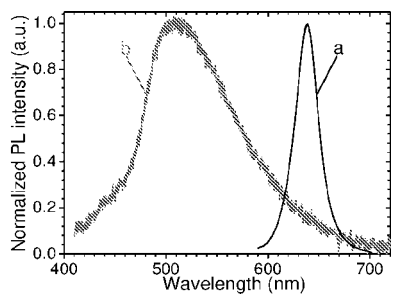

Figure 5. PL emission spectra of QDs in water before (a) and after (b) hydrothermal treatment for 8 hours at a temperature of 300 °C and a pressure of 40 MPa.

Second Quarter

The second quarter research activities in this subtask (2.4) were driven by the results of oxidation/stability studies of the last quarter. There we found that while we were able to preserve the optical properties under the harsh temperature/pressure conditions that simulate an EGS reservoir, the emission wavelength blue-shifted, indicative of severe surface oxidation. Since surface oxidation "destroys" part of the active CdSe quantum dot compound, for long-term application of our quantum dot tracers this oxidation process must be kept at a minimum. Therefore, we re-investigated our surface coating process in the search for a better glass-like silica compound layer with improved oxidation stability.

We investigated several new silica precursor compounds in terms of the stability of the formed glass-like protection layer around the quantum dots. The silica precursors investigated were triethoxymethylsilane (TEMS), 3-aminopropyl trimethoxysilane (APTS), 3-mercaptopropyl trimethoxysilane (MPTS), tetrabutyl orthosilicate (TBOS) and tetramethyl orthosilicate (TMOS). Surface coating layer formation around quantum dots was optimized individually for all of these precursors before the resulting layer stability was studied and compared to the previously used tetraethyl orthosilicate (TEOS) precursor.

To obtain initial insights into the sample stabilities of the various precursor without the need to conduct time- and resources-consuming hydrothermal experiments at each synthesis step, two fast and simple stability studies were conducted: 1) Structural stability of the individual silica-coated quantum dots was investigated after centrifugation of quantum dot samples in solution. Centrifugation studies give insite into the clustering trend of coated quantum dots, since clustered dots settle faster and are removed from solution. Clustering and other structural changes are important factors since they would significantly alter the diffusive behavior of quantum dot tracers. 2) The second type of stability studies focused on the optical properties of the samples. These studies were contacted under UV light illumination—UV light causes accelerated photo-induced oxidation and thus simulates harsh oxidation conditions such as those in EGS reservoirs. The outcomes are given in Figure 6 and clearly demonstrate that the MPTS precursor gave the best centrifugation results with nearly 100% stability (Figure 6a). In addition, this precursor also showed excellent behavior in long-term photo-oxidation studies, indicated by optical properties that stayed unchanged over days of UV light treatment (Figure 6b). In the next steps we will fabricate large amounts of quantum dot samples with silica coating synthesized from MPTS precursors and conduct hydrothermal experiments as described in the first quarter report (see above).

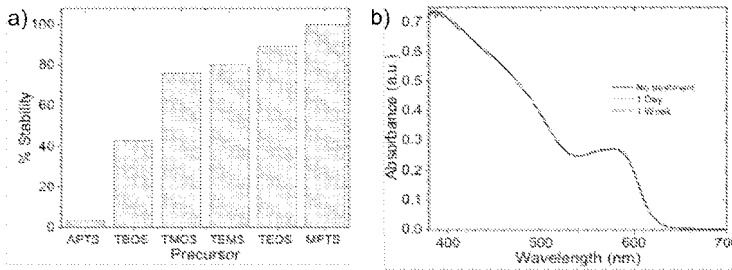

Figure 6. a) Structural stability studies showing percentage of quantum dots still in solution (un-clustered) after a centrifugation at 14500 rpm. b) Optical properties of quantum dots at various stages of the oxidation stability studies.

Third Quarter

The best silica-coated quantum dot samples (optimized in quarter 2; see above) were subjected to heat and pressure treatment to simulate EGS reservoirs (300 °C and a pressure of 40 MPa for 8 hours). The most important conclusion of these studies was that the silica coating of the quantum dots is too reactive at these high temperatures. In detail, the silanol moieties at the silica/quantum dot (QD) surface (QD-[Si-OH]x) are still active and can cross-link different quantum dots in a condensation reaction to form QD-[Si-O-Si-QD]x units (with x = 1, 2, 3 …). This uncontrolled cross-linking leads to precipitation; and while individual quantum dot units could be stable at these conditions, their cross-linking leads to formation of large clusters that are not soluble in aqueous environments, and eventually, loss of any quantum dot tracer species in solution occurs. This outcome forces us to re-design our quantum dot tracers.

In our next-generation quantum dot tracers we plan to replace the highly reactive silica shell with a single layer of bi- or tri-functional molecules. One of the functionalities will be chosen to bind to the quantum dot surface, whereas the other functionality has a very low affinity for quantum dots but will render them water-soluble. Our first synthetic efforts focused on two types of molecules: mercaptopropionic acid and citric acid. It should be mentioned that both of these molecules were already considered in our original proposal as potential surface ligands (coatings); however, (1) due to the initial successes using silica and (2) since these molecules require CdSe/CdS or CdSe/ZnS core-shell quantum dots, they were not further investigated until now.

Meanwhile, we have synthesized core-shell quantum dot samples with both types of surface ligands. Both samples show excellent water-solubility. Furthermore, for the core-shell quantum dot samples, luminescence is preserved after the surface-coating (ligand) exchange process (a schematic for exchange with mercaptopropionic acid is given in Figure 7). These samples are currently subjected to systematic high-temperature/pressure studies. To continuously optimize the sample properties and stability, we will perform these studies by step-wise increase of the temperature of the simulated EGI reservoir from 150 to 300 °C. This will give us better insights

into the stability behavior and should also allow us to distinguish between performance decay due to oxidation and precipitation—a differentiation that, unfortunately, was not possible for the silica sample due to their oxide nature.

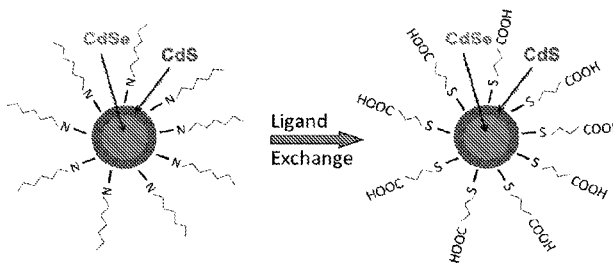

Figure 7. Schematic showing ligand exchange of core-shell CdSe/CdS samples with the water-soluble molecules mercaptopropionic acid.

Fourth Quarter

Activities in the 4th quarter included testing water-soluble quantum dots in simulated EGI reservoirs at initial temperatures of 150 °C and exploring direct synthesis methods of citric acid and mercaptopropionic acid stabilized quantum dots (see also previous quarter). Testing of the quantum dots revealed structural stability of the quantum dot cores; no oxidation and dissolution was detected by optical spectroscopy studies. However, we also observed unwanted clustering of the quantum dots, resulting in precipitation over prolonged times of heat treatment. Since clustering and partly precipitation would change the tracing characteristics of quantum dots, we are currently focusing our efforts on gaining insights in to the nature of clustering and develop solutions. A central question is whether clustering is caused by the surface ligands or the quantum dot surface (surface charge build-up). We are testing the temperature stability and reactivity of ligands currently employed and also of other types of potential ligand candidates. We conduct these studies by comparing mass spectroscopy and NMR spectroscopy results before and after the temperature treatment. So far, we found mercaptopropionic acid ligands are prone to dimerization due to the reactivity of the mercapto groups to form disulfide bonds. Citric acid ligands did not show dimerization tendency and we will focus future quantum dot temperature studies on samples with this type of ligand.

The defining goal for the next quarter will be to synthesize and test a soluble quantum dot that can survive at least 150 °C for one week in an autoclave with no structural degradation and reduction in solubility.

Phase 2, Subtask 2.5: Characterize the flow properties of the second-generation nonsorbing quantum dot tracers under ambient conditions

This subtask was deferred.

Phase 2, Subtask 2.6: Using a benchtop flow reactor, test the performance of the second-generation nonsorbing quantum dot tracers under conditions that simulate an injection/backflow test in an EGS wellbore

Approach

The flow reactor that was adapted in task 2.1 to simulate a newly sheared fracture will again be used to characterize the performance of the second-generation quantum dot tracers in an injection/backflow experiment. The experiment will involve injecting a solution of quantum dot tracers, followed by a shut-in phase, followed by a production phase—all at elevated temperature and pressure. Data from the experiment will be used to calibrate the numerical injection/backflow model.

Third Quarter

The design of the injection backflow reactor has been conducted in a way to maximize the amount of information that can be collected for each experiment, in addition to providing a platform conducive to the implementation of potential future experiments (see Figure 8). Flush and tracer solutions will be available at the inlet, while a three way valve will be used to control the direction of the flow through the reactor. Heating coils will bring the solutions to reservoir temperatures prior to their injection into the reactor. The reactor itself is 40" long and has a 2" ID, adequate for the minimization of boundary effects based on 400-600 μm diameter sand grains. Along the length of the reactor there will be six measurement ports, two at each entrance/exit and two in the middle. These will make it possible to make pressure and temperature measurements *in situ* and allow better control over reservoir conditions in the reactor. Furthermore, the reactor itself will be set up in such a way that its orientation can be controlled so that future experiments can be conducted at 0, 45, and 90 degree angles. The effluent will then be cooled and run through a flow cell for inline fluorescence measurements of conservative and reactive tracers. An Ocean Optics spectrometer was chosen because of the adequate resolution and particle detectability it provides, as well as superior versatility that can be used for future experiments in injection-backflow (and other) experiments.

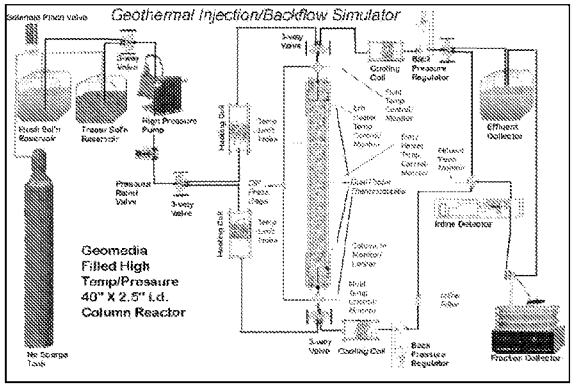

Figure 8. Schematic of the injection/backflow reactor.

Fourth Quarter

The injection/backflow reactor construction is progressing. One significant aspect that we have incorporated into its capabilities has been to change the design such that experiments will be able to be replicated in different orientations in relation to gravity (column can be rotated). This modification will allow for experiments to test that the quantum dot colloid transport is independent of fracture orientation. The large pieces that we have obtained are: a 2-liter high-temperature reaction vessel, a pump, a spectrometer, a lamp, a computer, and the data acquisition module. We are constructing the supporting and safety systems and anticipate starting to plumb the system together in order to perform some preliminary test runs during the next quarter.

Phase 2, Subtask 2.7: Modify the surfaces of the nonsorptive quantum dot tracers to render them sorptive; Update and calibrate the numerical model

Approach

Positively charged ligands bonded to the surface of the quantum dot tracers would provide for reversible sorption on negatively charged geothermal rocks. Likewise, scale inhibitors such as polycarboxylates, polyacrylates, and polymaleic anhydrides have been shown to sorb strongly but still reversibly within geothermal wellbores and formations. If these species are bonded to the quantum dots, they will render them reversibly sorptive on EGS formations, while retaining all of the fluorescence properties already developed and demonstrated. In this task we will explore techniques to modify the surfaces of the quantum dot tracers to render the quantum dots reversibly sorptive on EGS formations. A small portion of this task will also be devoted to extending the capabilities of the numerical model to provide surface area estimates from sorbing tracer breakthrough curves in single-well tracer tests (or, more specifically, from the differences in breakthrough curves of sorbing and nonsorbing tracers). Note that some of these capabilities

may also be developed under Task 2.2 if quantum dot tracers exhibit sorbing behavior in the flow reactor tests.

Figure 9 below is a Gantt chart showing the expected start and completion dates of each of the subtasks throughout the three years of the project.

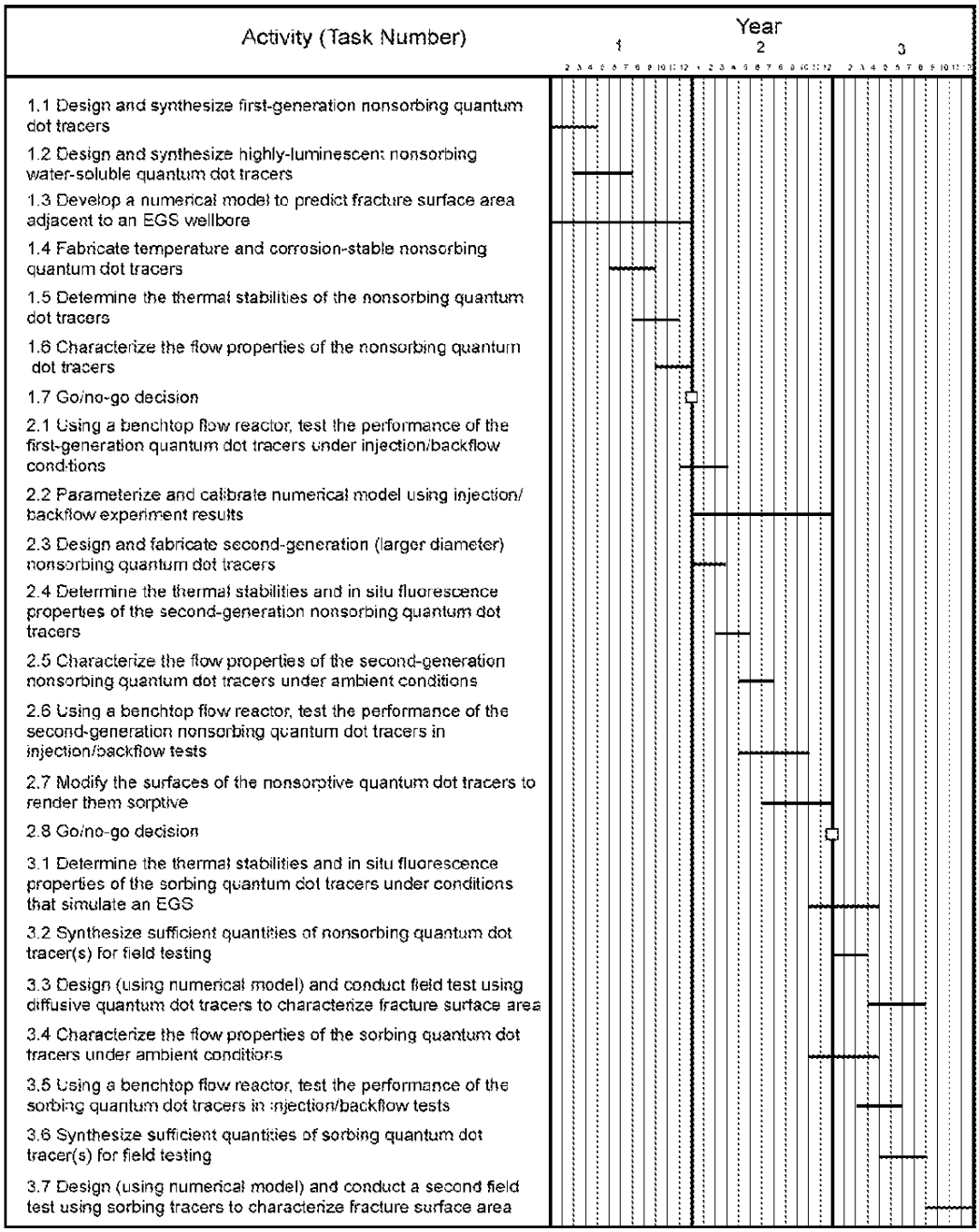

Figure 9. Gantt chart summarizing the Project Management Plan.

Phase II, Year 3

Progress Report for Year Ending September 30, 2012:

Quantum Dot Tracers for Use in Engineered Geothermal Systems

DE-EE0002768

Peter Rose[1], Principal Investigator; Michael Bartl[2], Co-Investigator; Paul Reimus[3], Co-Investigator; Jacqueline Siy[2], Mike Mella[1], Kevin Leecaster[1], Bridget Ayling[1], Eric Brauser[1], Vince Vermeul[4], Mark Williams[4], and Susan Petty[5]

[1]EGI, University of Utah
[2]Department of Chemistry, University of Utah
[3]Los Alamos National Laboratory, Los Alamos
[4]Pacific Northwest National Laboratory
[5]AltaRock Energy Corporation

Table of Contents for Phase II, Year 3

Project Objectives

The objective of this project is to develop and demonstrate a new class of tracers that offer great promise for use in characterizing fracture networks in EGS reservoirs. From laboratory synthesis and testing through numerical modeling and field demonstrations, we will demonstrate the amazing versatility and applicability of colloidal quantum dots as conservative (nonreactive) tracers. Through modifications of surface properties and diameters, they will then be transformed into reactive tracers that will sorb and diffuse in predictable ways with fracture surfaces and thereby be used to determine fracture surface areas.

Phase 3, Subtask 3.1: Design and fabricate second-generation nonsorbing quantum dot tracers

Approach

Quantum dot tracers were developed and demonstrated as originally proposed and all milestones were met. Most notably, the quantum dots survived an 8-hour test at 300°C under reducing (geothermal) aqueous conditions, resulting in an increase of their luminescence by a factor of three. However, as reported at the 2012 DOE Program Review, an unanticipated problem has been the long-term stability under room-temperature, oxidative conditions. This problem has resulted from an inadequate ligand chemistry that has caused the colloidal nanoparticles to coalesce and precipitate from solution. New ligand chemistry is being designed to provide for long-term room-temperature stability under oxidative conditions.

Second Quarter

Jacqueline Siy-Ronquillo and Eric Brauser

We have continued with the synthesis efforts from last quarter to produce water soluble CdSe/CdS "core-shell" quantum dots using sodium citrate as the stabilizing ligand. By modifying the adapted synthesis method, we are now able to produce quantum dots that display efficient photoluminescence or have bright color emission immediately after the synthesis. This eliminates the necessity for any post-synthesis treatment, such as irradiation by fluorescent or UV light which leads to quantum dot degradation by photo-oxidation. Some of these modifications include optimizing the amount or concentration of the thioacetamide used in the reaction, preventing air exposure during the "shell" addition and formation, and freshness of the "core" solution before "shell" addition.

Third Quarter

Jacqueline Siy-Ronquillo, Eric Brauser and Michael Bartl

Based on the successful synthesis method of core-shell CdSe/CdS quantum dots in the previous quarter, we further optimized the reaction conditions and used a low-temperature-oil-bath method rather than the microwave method that we initially used. As a result, we found that increasing the cadmium concentration in the low-temperature-oil-bath synthesis significantly increases the luminescence brightness of the quantum dots. We also found that the luminescence

intensity is sensitive to the solution pH at various points during the synthesis (i.e. during quantum dot core nucleation and growth).

Furthermore, we found that post-synthesis purification of samples by acetone precipitation and re-dissolution in water reduces un-wanted trap states ("dark states") that do not contribute to band-edge luminescence. In combination with addition of fresh citrate ligands after purification, we observed that the quantum dots are stable in dark, aqueous environment for long periods of time. However, it is important to note that multiple acetone treatments can reduce the overall brightness of the quantum dots. This is to be expected since it is known that purification causes the stripping off of some of the protective ligands on the quantum dot surface causing a lower luminescence yield.

We also started to investigate routes to scale up our quantum dot synthesis method from the current 50-milliliter-per-synthesis run (lab scale) to liter scale and, eventually, to hundreds-of-liter scale for field testing. We are glad to report that first scale-up tests were very successful. We demonstrated a 10-fold increase in synthesis volume without loss of the high quality and stability of quantum dots. The quantum dots had bright luminescence in the green-yellow part of the visible spectrum (555-565 nm wavelength emission).

Fourth Quarter

Jacqueline Siy-Ronquillo, Eric Brauser and Michael Bartl

In the previous quarter, we showed successful synthesis of a wide range of water soluble core-shell CdSe/CdS quantum dots with photoluminescence emissions from green to red and narrow size distribution using our modified low temperature oil bath method. This quarter we focused on scaling up the synthesis method as well as adding a silica layer to the quantum dots to make them more thermally stable. However, purification and stability of the silica-capped quantum dots proved to be very challenging because they formed a gel over time. This is possibly due to two reasons:

a. Cross linking of excess silica that was not removed during purification and/or,
b. Crosslinking of silica capping the core-shell quantum dots.

The quantum dots also lost significant photoluminescence brightness during the process. Because of these challenges, we decided to synthesize silica-capped core-shell quantum dots using a different route.

In this new method, we used initially hydrophobic core-shell CdSe/ZnS quantum dots, incorporated these quantum dots into silica spheres using a reverse microemulsion method developed by Nann et al. which changes it into water soluble quantum dots. The synthesized water soluble silica-capped quantum dots (CdSe/ZnS-SiO_2) have been stable at room temperature for over a month now. They have retained their original optical properties after the capping process as shown in Figure 1 below. There is no observable shift in the photoluminescence peak maximum indicating that the original size of the quantum dots is maintained. There is also no observable significant change in the photoluminescence full-width-at-half-maximum indicating that the size dispersion was maintained after the capping process.

Furthermore, the silica-capped quantum dots have retained the photoluminescence brightness of the original core-shell sample. These quantum dots were then subjected to hydrothermal stability tests.

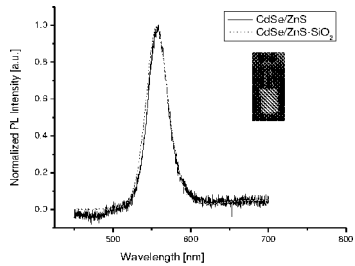

Figure 1. The emission spectra of purified CdSe/ZnS and CdSe/ZnS-SiO_2 (picture in the inset) quantum dots.

Phase 3, Subtask 3.2: <u>Determine the thermal stabilities and in situ fluorescence properties of the non-sorbing quantum dot tracers under conditions that simulate an EGS reservoir</u>

Approach

Using batch autoclave reactors, the candidate sorbing quantum dot tracers will be screened for thermal stability under conditions of temperature, pressure and chemistry that simulate a hydrothermal environment. For each tracer that survives the screening, its thermal decay kinetics will be determined using previously established methods. Likewise, the in situ fluorescence of each tracer at high temperature will be determined.

Accomplishments

First Quarter

Eric Brauser and Jacqueline Siy-Ronquillo:

Water-soluble "core/shell" quantum dots have been synthesized using sodium citrate as the stabilizing ligand, thioacetamide as the sulfur source for the shell material, and selenourea and cadmium perchlorate as the monomers for the core synthesis. These samples do not display any fluorescence immediately following synthesis. After four hours in an autoclave reactor at 150°C, samples showed no apparent agglomeration or structural breakdown, but do not display any change in luminescence. Irradiation by fluorescent or UV light has been shown to lead to very large gains in photoluminescence. It has been proposed that oxidation of surface atoms creates a

shell that passivates surface defects, increasing the luminescence. After weeks of irradiation these quantum dots eventually precipitate, resulting in a loss of all fluorescence.

Quantum dot samples were synthesized using the procedure above. They were then irradiated for 1-4 days and exhibited photoluminescence without visible precipitation. Autoclave tests of these quantum dots at 150 ℃ resulted in a redshift of the fluorescence maxima, which is attributed to quantum dot growth due to excess monomer precursors present in solution. Experiments to purify the quantum dot samples are being pursued in order to obtain quantum dots whose spectra do not change in high temperature environments. Furthermore, no luminescence gains have been observed in 150 ℃ tests of non-luminescent samples (those that have been synthesized but not irradiated).

Second Quarter

Jacqueline Siy-Ronquillo and Eric Brauser:

Due to degradation of the particles during irradiation, our focus for obtaining thermally stable quantum dots has returned to a reexamination of our synthesis approach. Whereas they are brightly fluorescent, these irradiated particles precipitated very easily and are not good candidates for reservoir tracers. From variations in the method previously described, it was found that the quantum dots' luminescence is sensitive to the pH and sodium citrate concentrations. Furthermore, purification of synthesized particles to remove excess monomer precursors resulted in highly monodisperse samples, as shown by the spectrum in Figure 2.

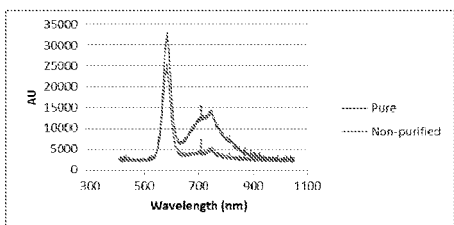

Figure 2. The emission spectra of purified and non-purified CdSe/CdS quantum dots

Our new approach results in quantum dots that show no loss of luminescence upon autoclave heating for 4 hours at 150 ℃ under reducing environment, as shown in Figure 3. Purification steps after the synthesis have been conducted and optimized to eliminate, or at least minimize, the problem of significant quantum dot growth and aggregation during the hydrothermal treatment. This is clearly shown in the minimal red-shifting of the photoluminescence spectra in Figure 3. Furthermore, the quantum dots produced in the modified method have better long term stability under room temperature, and even better if kept in dark places or in a refrigerator. They have stayed in solution for as long as two months now, showing no degradation in terms of its optical properties (absorbance and photoluminescence). We are proceeding with tests to confirm these results under harsher conditions.

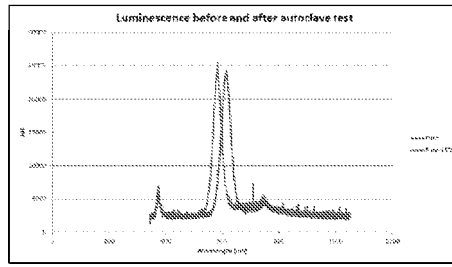

Figure 3. Photoluminescence emission spectra of CdSe/CdS quantum dots in water before and after hydrothermal treatment for 4 hours at 150 °C showing no loss in luminescence.

Current efforts focus on two aspects. First, we want to be able to modify or refine the synthesis method further in order to have better control and flexibility on the size of quantum dots produced. Currently, we are only able to synthesize "core-shell" quantum dots that emit in the red region. The goal is to be able to produce the same good quality quantum dots that emit in the entire visible spectrum (green, yellow, orange and red). Second, we want to extend the synthesis method to add another layer of coating to the quantum dots using any of the following: a) silica shell; b) amphiphilic ligand; c) combination of both silica shell and amphiphilic ligand. Based on literature reports, this addition can help the quantum dots achieve greater stability at higher temperatures and harsher conditions.

Third Quarter

Jacqueline Siy-Ronquillo, Eric Brauser and Michael Bartl

The third quarter activities in this subtask focused on testing the stability of the differently sized (and thus colored) quantum dots and investigating the impact of the modified synthesis method on the long-term stability of quantum dots in water at a temperature of 150 °C using a batch autoclave reactor.

The extended-time stability of quantum dots synthesized with our modified synthesis and purification method were tested. Samples were autoclave heated at 150 °C for 4, 8 and 12 hours. These new quantum dot samples showed great improvement. Whereas previous samples would strongly agglomerate and fall out of solution at times longer than 4 hours, the new samples showed very good stability even after 12 hours of heating.

Using the new low-temperature-oil-bath synthesis, coupled with the careful adjustment of synthesis conditions, gave us better control over the quantum dot size during synthesis. This resulted in producing luminescent water soluble quantum dot samples emitting over a wider range of the visible spectrum compared to before, now from green to red regions (see also Figure 4). The stability of the differently colored/sized quantum dots were tested by autoclave heating

for 8 hours at 150 °C under reducing environment. Figure 4 shows fours samples after the 8 hour testing at 150 °C. All four samples with green, yellow, orange and red colors still showed strong luminescence emission after the heat treatment. Moreover, the corresponding photoluminescence emission spectra reveal the shape of the emission peaks stayed narrow even after the heat treatment and the individual peaks are well separated, which will be of great importance for multi-color tracing applications.

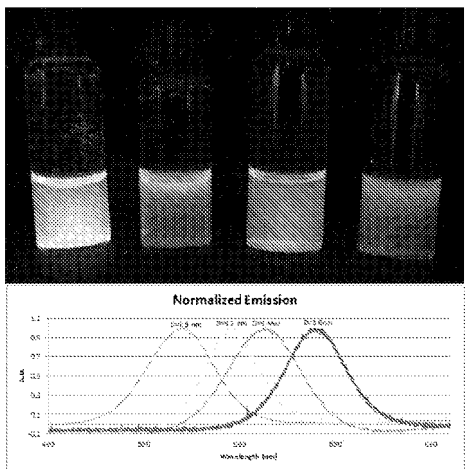

Figure 4. Photoluminescence emission images (top) and corresponding spectra (bottom) of CdSe/CdS quantum dots in water after hydrothermal treatment for 8 hours at 150 °C showing excellent multi-color luminescence properties.

Fourth Quarter

Jacqueline Siy-Ronquillo, Eric Brauser and Michael Bartl

The fourth quarter activities in this subtask focused on further optimizing quantum dot synthesis and testing their stability: We focused on two types of quantum dots: CdSe/CdS quantum dots synthesized in aqueous solution due to the simplicity of synthesis (see last quarter) and a new type of quantum dots based on CdSe/ZnS-SiO_2 multi-layer structures using the reverse microemulsion synthesis method (see below).

a) <u>CdSe/CdS Quantum Dots Synthesized in Aqueous Solution:</u>
Parameters of increased cadmium concentration and higher pH that were earlier discovered have a positive effect on to the brightness of synthesized quantum dots. Conditions investigated

included solution pH, cadmium concentration, injection volumes, and amount of added sodium citrate. All quantum dots synthesized were between 2.5 and 2.9 nm in diameter. Increasing the cadmium concentration consistently creates the highest luminescence, although at the lower range of pH 9, the polydispersity of the sample is evident in the absence of a characteristic absorbance peak. At pH 10 and 11, however, the absorbance peaks are distinct while the luminescence peaks benefit from a slightly larger addition of sodium citrate ligand. Doubling and halving the injection volumes alters the concentration by about a factor of two (2.1 μM and 1.1 μM, respectively), but the size is less affected (3.0 nm and 2.0 nm diameter).

Thermal stability testing: Quantum dots were synthesized with 0.08 M initial cadmium concentration and a molar ratio of 8:1:1 Cd:Se:S, at pH 10, as per previous successful syntheses. The resulting quantum dots were purified and then separated into four aliquots of 10 mL. To these were added 0, 10, 20, and 30 mg sodium citrate dehydrate. The samples were sonicated and then transferred to the ampoules for thermal study. The thermal conditions were 22, 30, and 48 hours at 150 C. All of the samples showed evident luminescence after 22 hours, but only the sample with 30 mg citrate showed luminescence after 30 hours. All samples were quenched at 48 hours. In addition, redshift of the luminescence peaks was observed, which suggests QD growth, though it is difficult to corroborate this with the absorbance spectra due to degradation of the characteristic peak after being exposed to high temperatures.

b) CdSe/ZnS-SiO_2 Multi-Layer Quantum Dot Structures:
These quantum dot samples were synthesized using the reverse microemulsion method. These core-shell-shell structures have a silica protective layer. It should be emphasized that we investigated a similar structure earlier in the research project. These nanocrystals showed an increased stability; however, they were prone to cross-linking and un-wanted precipitation due to the high reactivity of the silica shell. In the current approach we are using a microemulsion synthesis technique. This technique creates a denser silica shell and, importantly, the reactivity of the silica shell is strongly reduced; this prevents uncontrolled crosslinking and increases the quantum dot stability in solution.

The long term stability of these quantum dots in water was investigated using the same experimental conditions as in previous tests (same pretreatment of argon gas purging before sealing the samples in ampules, hydrothermal treatment at a temperature of 150 °C using a batch autoclave reactor under a reducing environment) to be able to compare their stability over previous samples (core shell quantum dots without silica coating).

The quantum dot sample was autoclave heated at 150 °C for 14 hours. The new quantum dot sample showed great improvement in its stability. Figure 5 shows the optical properties of the sample after 14 hour testing at 150 °C. Its corresponding photoluminescence emission peak stayed narrow, indicating that there was no change in size dispersion resulting from the hydrothermal process. The emission peak center wavelength did not shift significantly (red shift of only 6 nm), indicating a stable quantum dot size (no dissolution). In addition, there is no significant loss of luminescence intensity observed. Overall, these results show the improved thermal stability of the silica-capped core shell quantum dots over previous samples.

Interestingly, although the silica-capped quantum dots still have a high emission after the thermal treatment, it was observed that the sample pretreatment (purging with argon gas before sealing the ampules containing the sample) caused a significant decrease in the emission intensity as compared to un-purged quantum dots. It can be seen from the figure that prior to pretreatment for the hydrothermal treatment, the quantum dot sample has a higher intensity and visibly brighter emission than both the autoclave control and the autoclaved sample. Because the optical properties of the autoclaved sample did not change significantly compared to the control after the hydrothermal treatment, it can be concluded that the loss is due to the pretreatment process. It was also observed that the measured pH of the quantum dot samples decreased from 7 to 5 after the pretreatment (purging) process. This can explain the decrease in the emission intensity of these samples from the original and corresponds with results from previous quarter, which showed that the photoluminescence intensity of quantum dots is sensitive to solution pH.

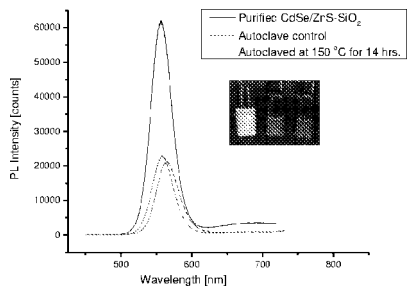

Figure 5. Photoluminescence spectra and emission (inset from left to right) of purified water soluble CdSe/ZnS-SiO_2 pretreated/purged CdSe/ZnS-SiO_2 (autoclave control), pretreated/purged CdSe/ZnS-SiO_2 hydrothermally treated for 14 hours at 150 °C under reducing environment (autoclaved sample).

We will work on solving this problem in the next quarter. Our approach will be to add a layer of polyethylene glycol (an inexpensive polymer) around the silica. This polymer is known to form a protective layer and should make the quantum dots stable to pH changes.

Phase 3, Subtask 3.3: <u>Characterize the flow properties of the sorbing quantum dot tracers under ambient conditions</u>

Accomplishments

First Quarter

As described above, no samples of quantum dots were available for testing. Instead, polystyrene nanospheres having diameters of 20 nanometers were purchased and used in flow tests as surrogates for the quantum dots. A solution of polystyrene nanospheres and 1,5 naphthalene disulfonate (1,5 nds) as a conservative tracer was prepared in an aqueous solution, which had flowed through the Ottawa sand column in order to saturate it in silica. The solution was then adjusted to a pH of 8.5 and pumped through the sand column at ambient temperature.

Figure 6a shows a plot of the concentrations of solute tracer and polystyrene nanospheres upon elution from the sand column. The polystyrene nanospheres took almost two hours longer than the 1,5-nds to reach a constant elution concentration. Figure 6b shows the effect of flushing the column with tracer-free water. The polystyrene nanospheres concentration began to drop slightly before the 1,5-nds concentration began to drop during the flushing experiment, but fell more slowly than the conservative tracer. The final shift in polystyrene nanosphere concentration is likely due to detector shift.

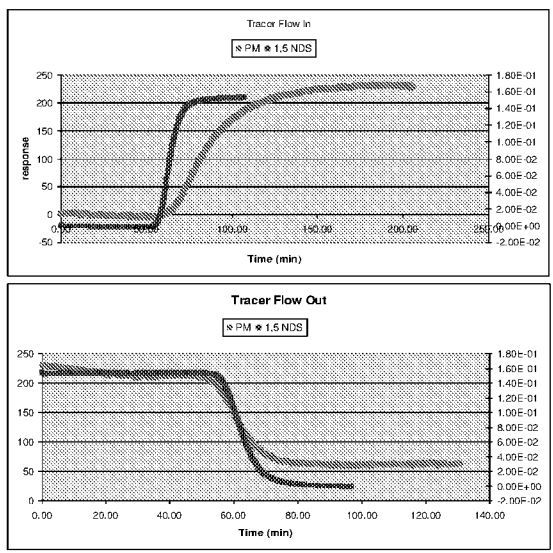

Figure 6. (a) Concentration of polystyrene nanospheres and 1,5-nds (solute) tracer after elution from a sand-packed column at ambient temperature. At t = 0, a valve was switched allowing the solution containing the tracers to flow into the column. (b) At t = 0, the valve was switched again, allowing tracer-free water to flow through the column, flushing the tracers from the column.

Fourth Quarter

Eric Brauser:

A 500 mL sample of brightly luminescent quantum dots with mean diameter of 3.5 nm and an emission wavelength of 561 nm were synthesized. The sample showed good benchtop stability of at least one month. The quantum dot solution was used to dissolve 1,5-napthalene disulfonate to make a 100 ppm solution of conservative tracer with the solution of highly luminescent quantum dots. The solution was then used as a proof-of-concept experiment demonstrating the behavior of quantum dots in a porous medium.

A column of Ottawa sand with grain sizes between 450-500 μm was used to simulate a reservoir environment. The tracer solution was then constantly pumped through the column until both the 1,5-NDS and quantum dots showed up in the effluent before being flushed with tracer-free deionized water. The solutes were detected using in-line absorbance and fluorescence spectrometers detecting 310 nm absorbance and 561 nm emission wavelengths. Figure 7 shows the normalized concentration breakthrough curves of the 1,5-NDS and the quantum dots. The quantum dots reach a steady effluent concentration approximately 50 minutes after the conservative tracer.

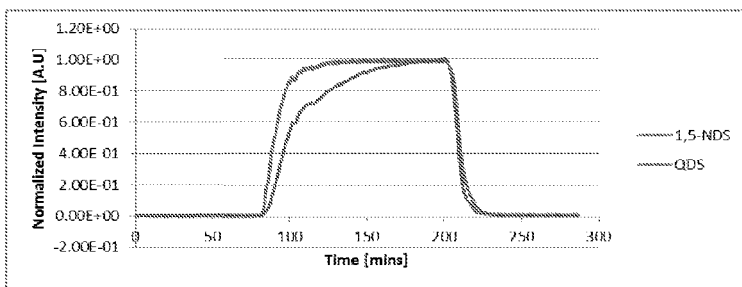

Figure 7: Breakthrough curves of conservative tracer 1,5-NDS and quantum dots

Near term follow-up will deal with the elimination of detector shift and intensity variation over the course of a single experiment. With stability in the detectors, the focus of the experiment can then move to developing calibration curves for quantum dot limits of detection, performing pulse injections, and comparing quantum dot results with earlier polystyrene surrogates. Long-term goals include column heating to represent geothermal media and modeling colloidal transport via numerical methods.

Phase 3, Subtask 3.4: Using a benchtop flow reactor, test the performance of the sorbing quantum dot tracers under conditions that simulate an injection/backflow test in an EGS wellbore

Approach

The design of the injection backflow reactor has been conducted in a way to maximize the amount of information that can be collected for each experiment, in addition to providing a platform conducive to the implementation of potential future experiments (see Figure 8). Flush and tracer solutions will be available at the inlet, while a three way valve will be used to control the direction of the flow through the reactor. Heating coils will bring the solutions to reservoir temperatures prior to their injection into the reactor.

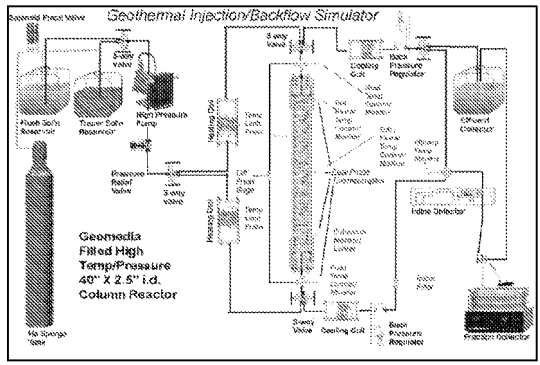

Figure 8. Schematic of the injection/backflow reactor.

The reactor itself is 40" long and has a 2" ID, adequate for the minimization of boundary effects based on 400-600 μm diameter sand grains. Along the length of the reactor there will be six measurement ports, two at each entrance/exit and two in the middle. These will make it possible to make pressure and temperature measurements *in situ* and allow better control over reservoir conditions in the reactor. Furthermore, the reactor itself will be set up in such a way that its orientation can be controlled so that future experiments can be conducted at 0, 45, and 90 degree angles. The effluent will then be cooled and run through a flow cell for inline fluorescence measurements of conservative and reactive tracers. An Ocean Optics spectrometer was chosen because of the adequate resolution and particle detectability it provides, as well as superior versatility that can be used for future experiments in injection-backflow (and other) experiments.

Accomplishments

Second Quarter

Kevin Leecaster:

Progress was made on completing the injection-backflow reactor (see Figure 9).The preheaters were constructed and installed. The differential and absolute pressure gages were installed. All of the tubing and valves have been installed and connected. The four controllers and solid state relays for the heaters have been installed. A balance was installed under the solution vessels for measuring the mass flow rate into the reactor and the data acquisition center was attached to the reactor support structure. Components that have yet to be finished prior to initiating experimentation with the equipment are indicated in Table 1.

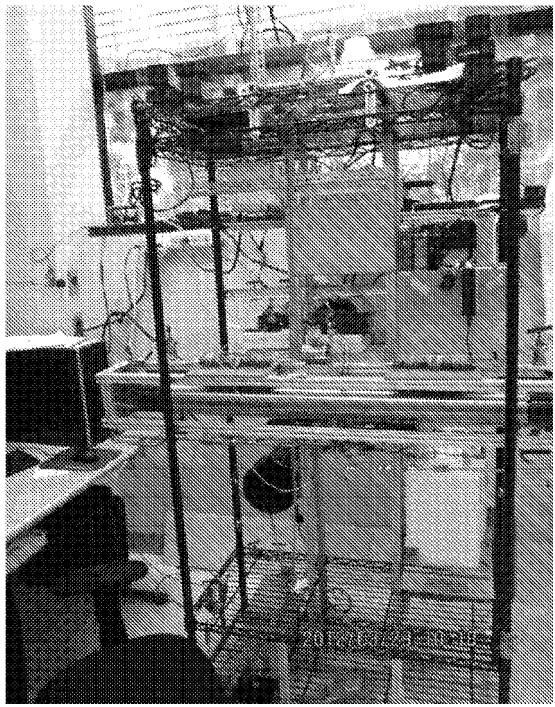

Figure 9. Photograph of the injection-backflow reactor.

Table 1. Components that remain to be completed on the injection-backflow reactor.

Component	Proportion Completed		Major Remaining Task	
	Mechanical	Electronic	Mechanical	Electronic
Support Structure	0.9	NA	Safety Enclosure Needs to be Hung on Hinges	
Axle system	0.8	NA	Angle Pin Installation	
Preheaters	0.9	0.8	Insulation	Connections
Column heaters	0.7	0.8	Insulation Removal to Fit into Cage	Connections
Sparging System	1	1		
Data Acquisiton System	0.9	.7	Breakout Box Backordered	Connections/Testing
In-line Detector	1	0.9		Connections/Testing
Effluent Cooler	.9	1	Fix Leak at Axle Entry	
Flow Rate Monitor	1	0.9		Software/Testing
Column Loading Stand	0.8	NA	Add Braces	
Column Loading System	1	NA		
Tubing	0.9	NA	Test/Tighten	
Fraction Collector	1	0.9		
Flow Switching Valves	0.9	NA	Insulation	
Temperature Monitors	0.9	0.9	Test/Tighten	Wiring
Pressure Monitors	0.9	0.9	Test/Tighten	Wiring
Pump	0.9	0.9	Rupture Disk Installation	Connections
Overall	0.9	0.88	Dead Volume Measurements & Pressure Testing	

Third Quarter

Kevin Leecaster:

The injection-backflow reactor is almost ready for the first experiments (Table 2). An issue with the EEPROM chip in the spectrometer was resolved this quarter. Its software has been tested and a method for using it has been developed. The pressure gages, thermocouples, and fraction collector have been connected to the data acquisition system. The column heaters have been adjusted and are ready to be installed after all of the dead volume pathways are measured. The sparging system has been connected to a timer allowing for moderate flow of He for two minutes each half hour during the work day with early morning longer periods optional. The pump has been tested and used to help with the pressure gage calibration and spectrometer troubleshooting.

Table 2. Injection-Backflow Reactor Construction & Testing Progress.

Component	Proportion Completed		Progress this Quarter	
	Mechanical	Electronic	Mechanical	Electronic
Support Structure	0.95	NA	Safety Enclosure Hinged	
Axle system	0.95	NA	Inclinometer Obtained	
Preheaters	0.95	1	Insulation	Connections Made
Column heaters	1	0.9	Insulation Removed to Fit into Cage	Connections Made
Sparging System	1	1	Working	Working
Data Acquisiton System	1	1	Breakout Box Received	Connections Made & Tested
In-line Detector	1	1		Connections Made & Tested
Effluent Cooler	1	1	Leak Fixed at Axle Entry	
Flow Rate Monitor	1	0.95		Tested
Column Loading Stand	0.95	NA	Braces Added, Strap needs Adjustment	
Column Loading System	1	NA	Tested	
Tubing	1	NA	Tested & Tightened	
Fraction Collector	1	1		Connected to DAQ
Flow Switching Valves	0.9	NA	Insulation still Required	
Temperature Monitors	0.9	1	Tested on Preheaters	Wired
Pressure Monitors	1	1	Tested	Wired & Calibrated
Pump	1	1	Rupture Disk Installed	Connections
Overall	0.95	0.95	Dead Volume Measurements & Pressure Testing	

We have begun to crush and sieve mineral samples for use as analogue geomedia. We currently have calcite, illite, anorthite, and two types of mafic basalt: massive and scoria. The two samples were qualitatively compared using XRD and the mineralogy of two rock samples are congruous in type to distinct geomedia with similar reactivity, but with different tortuosity, porosity, and surface area (Figure 10). Basalt is one of the next rock types with which we will experiment as it is a common host rock in geothermal reservoirs. Because of its position at the top of the Bowen's reaction series, it is hoped that some of the dissolution and associated pH complications encountered with quartz sands can be avoided.

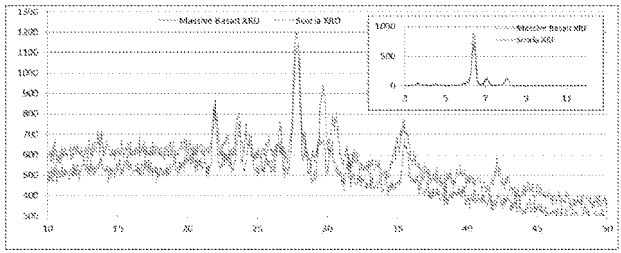

Figure 10: Results of X-ray diffraction and fluorescence analysis of scoria and massive basalt specimens obtained from Wards Natural Science, Inc. showing the similar mineralogy in the two samples.

Phase 3, Subtask 3.5: Design (using numerical model) an injection/withdrawal field test using sorptive quantum dot tracers as part of an EGS stimulation experiment to characterize the fracture surface area of the newly created heat exchanger

Accomplishments

First Quarter

Mark Williams (PNNL):

Numerical models are being developed using the ToughReact code for interpretation of the two-well tracer test conducted in September 2011 at the Soda Lake site and for investigation of the efficacy of using single-well injection/withdrawal tests at the site for fractured reservoir characterization. Site characterization and tracer parameters from fitting the two-well tracer test data are used for the single-well injection-withdrawal test models. The ToughReact code was selected to take advantage of the MINC option for simulating a fractured reservoir and options for simulating sorbing and thermally decay of tracers.

Current efforts have involved developing a preliminary two-dimensional model (constant thickness) for fitting the September 2011 Soda Lake tracer test with conservative (1,6 NDS) and reactive (Safranin-T, sorption with thermal decay) tracers. A slightly different two-dimensional plan-view model has also been developed for simulating single-well injection-withdrawal tests at the site along with a one-dimensional, radially symmetric, model (which is more computationally efficient and provides similar results). Results of these preliminary models are provided in the 2012 Stanford Geothermal Workshop paper ("Use of Tracers to Interrogate Fracture Surface Area in Single-Well Tracer Tests in EGS Systems," Paul REIMUS, Mark WILLIAMS, Vince VERMEUL, Peter ROSE, Kevin LEECASTER, Bridget AYLING, Raphael SANJUAN, Morgan AMES, Cynthia DEAN, and Dick BENOIT").

Continuing efforts include updating numerical models based on laboratory measurements of Safranin-T sorption with Soda Lake site materials and at reservoir conditions. This will help constrain estimates of fracture volumes / areas from fitting of the September 2011 two well tracer test data. Additional site characterization information will also be evaluated for inclusion in the site-specific model. Sensitivity studies will also be run to investigate impact of fracture spacing and volumes on test responses for evaluation of parameter uncertainty. This range of parameters will then be used to run a suite of single-well injection-withdrawal simulations for different operational scenarios to help design field tests where the field results would be useful for determining fracture spacing/area at a specific site. A preliminary example of the responses of a single-well injection-withdrawal test for two operational conditions (one hour tracer pulse vs. continuous tracer injection for three days) using the current fitting of site parameters from the two-well tracer test data is shown below (Figure 11).

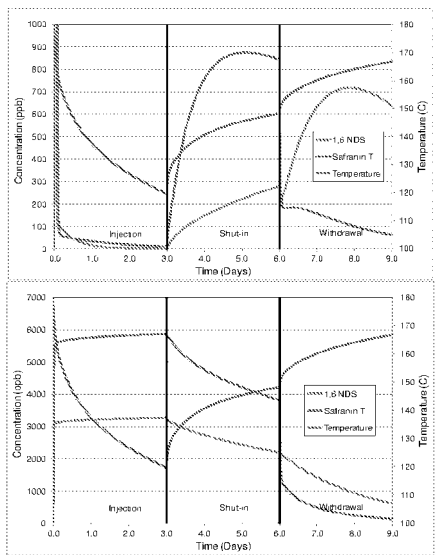

Figure 11. Single-Well Injection-Withdrawal Simulation. (a) 1 hour tracer pulse followed by fresh water during injection stage (b) constant tracer concentration during injection stage (same mass as a). Simulated concentrations and temperature in injection/withdrawal well.

Second Quarter

Mark Williams, PNNL:

Efforts for this subtask during this quarter focused on setting up sensitivity cases for investigating injection/withdrawal test responses to changes in fracture area and fracture volume using ToughReact simulations. These cases use the site parameters and tracer parameters from the preliminary fitting using ToughReact of the Soda Lake two well tracer test conducted in the fall of 2011 (1,6-NDS and Safranin-T). As shown in Figure 12a, increases in fracture area resulted in higher withdrawal stream temperatures (e.g. more fractures, higher fracture spacing); however changes only in fracture volume (e.g. only dilation of existing fracture apertures) did not have an impact on the withdrawal stream temperatures. These results are similar to the general conclusions of Pruess and Dougherty (2010) for using withdrawal temperatures for fracture volume determination from injection/withdrawal tests.

Tracer responses to changes in fracture surface area and fracture volume are shown in Figure 12b,c for a conservative tracer (1,6-NDS) and a sorbing/thermally decaying tracer (Safranin-T). Both sorption (reversible Kd) and thermal decay are simulated for Safranin-T in these ToughReact runs. These results show that the mass recovery of tracers from an injection/withdrawal test can be sensitive to both fracture surface area and fracture volume, but the recovery results would be site, tracer, and operationally specific. Work will continue on sensitivity cases using operational design, site parameters, and tracer parameters showing responses in tracer mass recovery. These models will also be updated from further work planned the Soda Lake two-well tracer test fit models and/or from new models developed as data become available from other geothermal test sites with other tracers of interest.

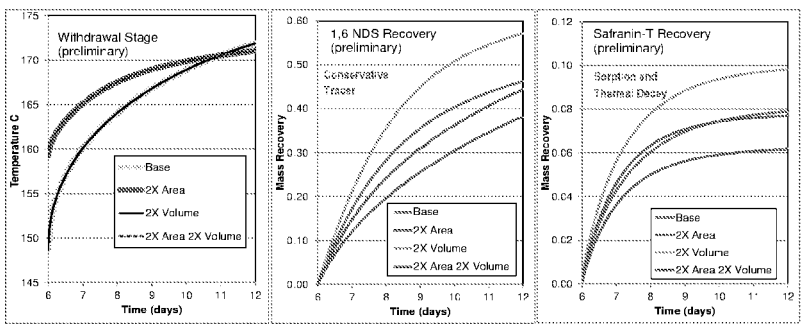

Figure 12. ToughReact simulation results showing impacts of changes in fracture surface area and fracture volume on the withdrawal stream temperatures and cumulative tracer mass recovery for the two different tracers. The withdrawal period follows (see Q1 plots) a 3 day injection period (constant concentration) and a 3 day shut-in period.

Paul Reimus, LANL:

Modeling sensitivity studies using the MULTRAN code were initiated to evaluate breakthrough curves that might be expected in both single-well and cross-hole tracer tests from quantum dot

tracers of different sizes and with different adsorption/desorption properties (relative to breakthrough curves of more conventional conservative solute tracers). The objective of this exercise is to evaluate optimal quantum dot tracer properties for interrogating various geothermal reservoir characteristics, or alternatively, to determine what reservoir characteristics can be best evaluated for a given set of quantum dot tracer properties.

Phase 3, Subtask 3.6: Synthesize sufficient quantities of sorbing quantum dot tracer(s) for field testing.

Approach

At this point, only very small quantities of nonsorbing quantum dot tracers will have been synthesized for the above described testing—quantities that are insufficient for any field demonstrations of tracer properties. For the quantum-dot tracers that have been shown to be sufficiently robust, a method will be developed to synthesize decagram quantities for testing in an EGS wellbore or reservoir. For three visibly fluorescing and one IR-fluorescing quantum dot tracer, 100 g of each will be synthesized.

Phase 3, Subtask 3.7: Conduct a field test using sorbing quantum dot tracers as part of an EGS stimulation experiment to characterize the fracture surface area of the newly created heat exchanger

First Quarter

No activities scheduled until the third quarter of FY2012.

Phase II, Year 3

Progress Report for Year Ending September 30, 2013:

Quantum Dot Tracers for Use in Engineered Geothermal Systems

DE-EE0002768

Peter Rose[1], Principal Investigator; Michael Bartl[2], Co-Investigator; Paul Reimus[3], Co-Investigator; Eric Brauser[1], Jeffrey Oates[1], Vince Vermeul[4], Mark Williams[4], and Susan Petty[5]

[1]EGI, University of Utah
[2]Department of Chemistry, University of Utah
[3]Los Alamos National Laboratory, Los Alamos
[4]Pacific Northwest National Laboratory
[5]AltaRock Energy Corporation

Table of Contents for Phase II, Year 3

Project Objectives

The objective of this project is to develop and demonstrate a new class of tracers that offer great promise for use in characterizing fracture networks in EGS reservoirs. From laboratory synthesis and testing through numerical modeling and field demonstrations, we will demonstrate the amazing versatility and applicability of colloidal quantum dots as conservative (nonreactive) tracers. Through modifications of surface properties and diameters, they will then be transformed into reactive tracers that will sorb and diffuse in predictable ways with fracture surfaces and thereby be used to determine fracture surface areas.

Phase 3, Subtask 3.1: Design and fabricate second-generation nonsorbing quantum dot tracers

Approach

First-generation quantum dot tracers were developed and demonstrated as proposed and all original milestones were met. Most notably, the quantum dots survived an 8-hour test at 300°C under reducing (geothermal) aqueous conditions, resulting in an increase of their luminescence by a factor of three. However, as reported at the 2012 DOE Program Review, an unanticipated problem has been the long-term stability under room-temperature, oxidative conditions. This problem has resulted from an inadequate ligand chemistry that has caused the colloidal nanoparticles to coalesce and precipitate from solution. New ligand chemistry is being designed to provide for long-term room-temperature stability under oxidative conditions.

First Quarter, 2013

Eric Brauser and Michael Bartl

The CdSe/ZnS-SiO_2 core-shell-shell quantum dots developed in the last quarter were further optimized in terms of surface reactivity and long-term stability. For this, the amount of silica coating and the time of ripening were varied. Lower silica concentrations were helpful in reducing the post-synthesis purification process, which is necessary mainly to remove unreacted silica that would cross-link quantum dots over time and precipitate them out of solution. With the optimized process, quantum dots have excellent solution stability and shelf lifetimes exceeding 1 month. We will further monitor and optimize shelf life together with high-temperature stability studies (see next section).

We also started with experiments to add a layer of polyethylene glycol (an inexpensive polymer) around the silica layer. This polymer is known to enhance stability of quantum dots toward pH changes. This process was necessary since we observed in the last quarter that pH changes during sample purging before high-temperature stability testing reduced the photoluminescence emission efficiency of quantum dots. So far, we have succeeded in attaching polyethylene glycol onto the silica layer; however, optimization of the amount and the polyethylene glycol chain length is needed, since we observed gelation of quantum dots into a viscous gel-like form.

Second Quarter, 2013
Task complete.

Phase 3, Subtask 3.2: Determine the thermal stabilities and in situ fluorescence properties of the non-sorbing quantum dot tracers under conditions that simulate an EGS reservoir

Approach

Using batch autoclave reactors, the candidate sorbing quantum dot tracers will be screened for thermal stability under conditions of temperature, pressure and chemistry that simulate a hydrothermal environment. For each tracer that survives the screening, its thermal decay kinetics will be determined using previously established methods. Likewise, the in situ fluorescence of each tracer at high temperature will be determined.

First Quarter, 2013

Eric Brauser and Michael Bartl

After the first successful autoclave tests at 150 °C last quarter on the CdSe/ZnS-SiO_2 core-shell-shell quantum dots, we performed new tests at both longer times and higher temperatures. To account for observed reduction in photoluminescence emission efficiency of quantum dots after argon gas purging (see last quarter report) all experiments were performed with two sets of samples: 1) samples for which the solution and the ampule atmosphere were purged with argon, and 2) samples for which only the ampule atmosphere on top of the solution was purged. We observed that regardless of the time and temperature of autoclave heat-treatment, the former samples showed lower emission efficiencies; highlighting the importance of the current polyethylene glycol studies (see previous section).

In the first set of experiments, samples were kept in the autoclave at a temperature of 150 °C for 24 hours (increased by ten hours from last quarter). Impressively, the samples retained their emission intensity; the longer time of heating, however, shifted the emission peak from the initial 560 nm to around 490 nm (still in the green range).

In the second set of experiments, the temperature of the autoclave heat-treatment was increased from 150 °C to 250 °C; and the samples were kept at this elevated temperature for 24 hours. While we observed the same shift of the emission peak to around 490 nm, most importantly, the samples retained their emission intensity even at these high temperatures.

These results are very encouraging. Currently we are investigating the emission peak shift to lower wavelength positions and we are exploring autoclave experiments at even longer times and higher temperatures.

Phase 3, Subtask 3.3: Characterize the flow properties of the sorbing quantum dot tracers under ambient conditions

Second Quarter, 2013

Eric Brauser:

Quantum dots (QDs) with diameter of 3.0 nm were pumped through a sand column at various flow rates. The detector responses were normalized and plotted against the volume of water or QD/1,5-NDS solution pumped into the column (see Figure 1). The QDs behave conservatively, based on the agreement of the response with the well-studied 1,5-NDS tracer. Small inconsistencies in the overall breakthrough time may have arisen from slight variations in the instantaneous flow rates created by the pump, which were observed by taking numerous average flow rates in 30-60 second time intervals at different times during the experiment.

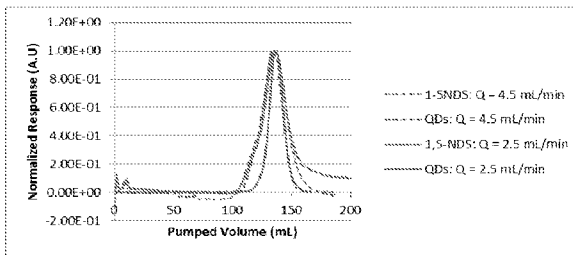

Figure 1. Plots of a quantum dot tracer co-eluting with a conservative solute tracer in sand-packed-column tests at 25°C.

The Q=2.5 mL/min experiment was then further analyzed by creating a calibration curve from diluted QD samples and correlating luminescence intensity with the QD concentration using previously developed semi-empirical models. Using earlier calculations of the initial QD concentration, found to be 3.1×10^{-6} mol/L, the total number of QDs injected for a 5 min pulse was calculated to be 2.3×10^{16} particles. Numerical integration of the concentration/time provided the total number of QDs that eluted from the column, found to be 5.1×10^{15} particles, giving a percent recovery of 77.8%.

Third Quarter, 2013

Eric Brauser:

The nature of QD retention was investigated by performing step-injection experiments and then analyzing the breakthrough curves and retention characteristics. QDs were injected in solution at a flow rate of 2.5 mL/min until they were visible in the effluent and their observed luminescence spectrum was stable, approximately 85 minutes. The column was flushed with deionized water between tracer injections. Figures 2 and 3 show the pure QD fluorescence spectrum overlaid on the stable luminescence spectrum of the effluent QDs. It is apparent that there is much less QD penetration through the column in the initial injection compared to the subsequent injection test. The percent recovery for these tests was obtained by numeric integration of the luminescence spectrum.

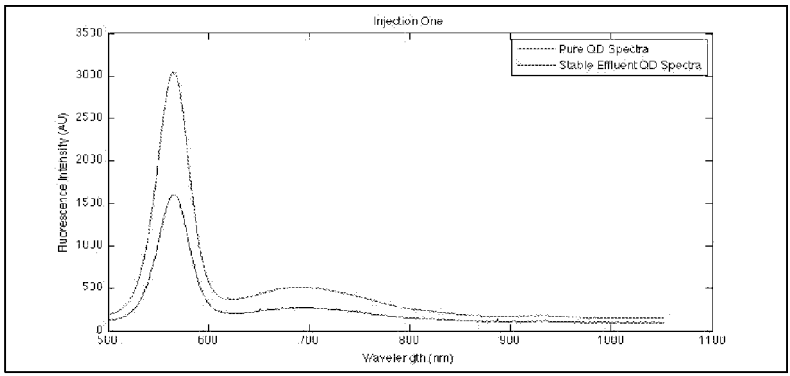

Figure 2: First injection of quantum dots

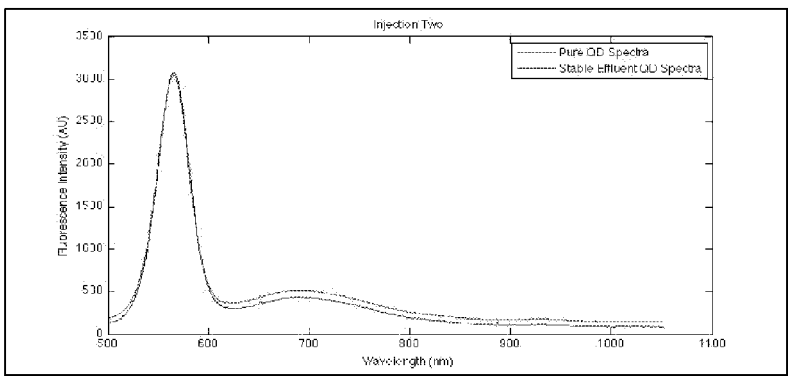

Figure 3: Second injection of quantum dots

For the first injection 77% of the QDs were recovered and in the second, 109% recovery was calculated, suggesting that QDs from the first test were withheld and continued to travel through the column and exit in the effluent. The recovery amounts reported in last quarter's report are similar to those of the first injection test, but are inconsistent with the second and require additional explanation. The dimensionless breakthrough curves in figures 4 and 5 were used with the CXTFIT code to estimate the partition coefficient in a two-region model. The modeling results reasonably follow the breakthrough behavior and predict an increasing partition

coefficient from injection one to injection two, indicating that the first QDs experience more of the immobile regions than those in the second injection.

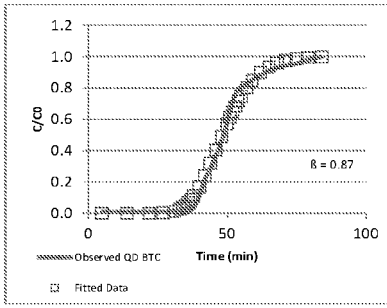

Figure 4: Plot of first injection modeled data

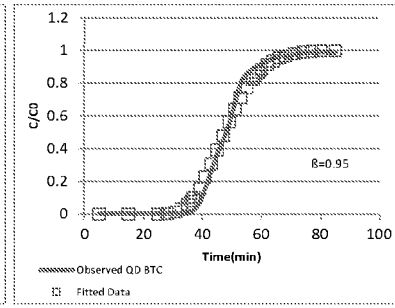

Figure 5: Plot of second injection modeled data

Fourth Quarter, 2013

Task complete.

Phase 3, Subtask 3.4: Using a benchtop flow reactor, test the performance of the sorbing quantum dot tracers under conditions that simulate an injection/backflow test in an EGS wellbore

Approach

The design of the injection backflow reactor has been conducted in a way to maximize the amount of information that can be collected for each experiment, in addition to providing a platform conducive to the implementation of potential future experiments (see Figure 6). Flush and tracer solutions will be available at the inlet, while a three way valve will be used to control the direction of the flow through the reactor. Heating coils will bring the solutions to reservoir temperatures prior to their injection into the reactor. The reactor itself is 40" long and has a 2" ID, adequate for the minimization of boundary effects based on 400-600 µm diameter sand grains. Along the length of the reactor there will be six measurement ports, two at each entrance/exit and two in the middle. These will make it possible to make pressure and temperature measurements *in situ* and allow better control over reservoir conditions in the reactor. Furthermore, the reactor itself will be set up in such a way that its orientation can be controlled so that future experiments can be conducted at 0, 45, and 90 degree angles. The effluent will then be cooled and run through a flow cell for inline fluorescence measurements of conservative and reactive tracers. An Ocean Optics spectrometer was chosen because of the adequate resolution and particle detectability it provides, as well as superior versatility that can be used for future experiments in injection-backflow (and other) experiments.

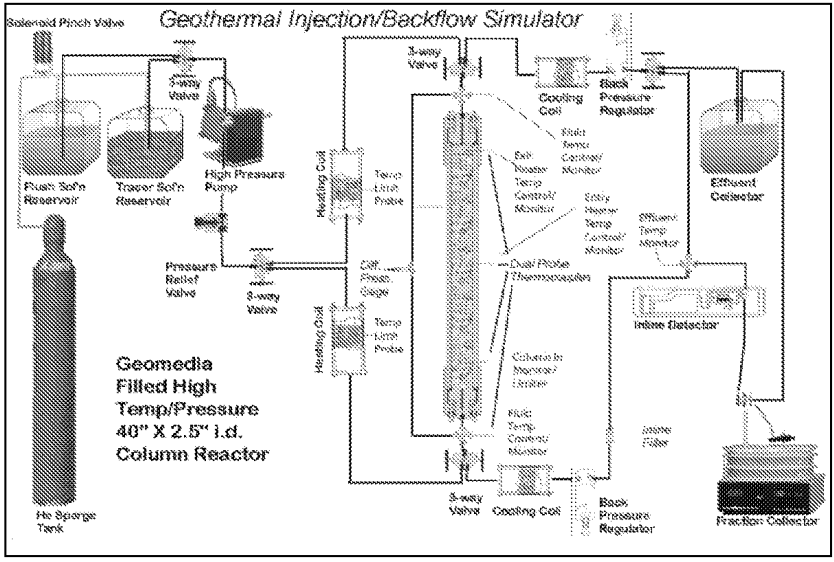

Figure 6. Schematic of the injection/backflow reactor.

Progress was made on completing the injection-backflow reactor (see Figure 7).The preheaters were constructed and installed. The differential and absolute pressure gages were installed. All of the tubing and valves have been installed and connected. The four controllers and solid state relays for the heaters have been installed. A balance was installed under the solution vessels for measuring the mass flow rate into the reactor and the data acquisition center was attached to the reactor support structure.

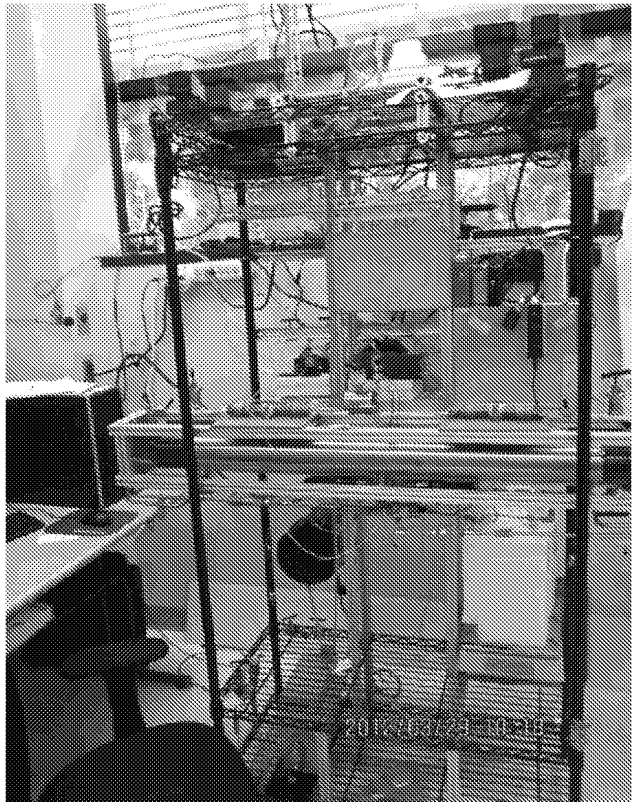

Figure 7. Photograph of the injection-backflow reactor.

Fourth Quarter, 2013

Task complete.

Phase 3, Subtask 3.5: <u>Design (using numerical model) an injection/withdrawal field test using sorptive quantum dot tracers as part of an EGS stimulation experiment to characterize the fracture surface area of the newly created heat exchanger</u>

Fourth Quarter, 2012

Mark Williams, PNNL:

Efforts for this subtask during this quarter focused on setting up sensitivity cases for investigating injection/withdrawal test responses to changes in fracture area and fracture volume using ToughReact simulations. These cases use the site parameters and tracer parameters from the preliminary fitting using ToughReact of the Soda Lake two well tracer test conducted in the fall of 2011 (1,6-NDS and Safranin-T). As shown in Figure 8a, increases in fracture area resulted in higher withdrawal stream temperatures (e.g. more fractures, higher fracture spacing); however changes only in fracture volume (e.g. only dilation of existing fracture apertures) did not have an impact on the withdrawal stream temperatures. These results are similar to the general conclusions of Pruess and Dougherty (2010) for using withdrawal temperatures for fracture volume determination from injection/withdrawal tests.

Tracer responses to changes in fracture surface area and fracture volume are shown in Figure 8b,c for a conservative tracer (1,6-NDS) and a sorbing/thermally decaying tracer (Safranin-T). Both sorption (reversible Kd) and thermal decay are simulated for Safranin-T in these ToughReact runs. These results show that the mass recovery of tracers from an injection/withdrawal test can be sensitive to both fracture surface area and fracture volume, but the recovery results would be site, tracer, and operationally specific. Work will continue on sensitivity cases using operational design, site parameters, and tracer parameters showing responses in tracer mass recovery. These models will also be updated from further work planned the Soda Lake two-well tracer test fit models and/or from new models developed as data become available from other geothermal test sites with other tracers of interest.

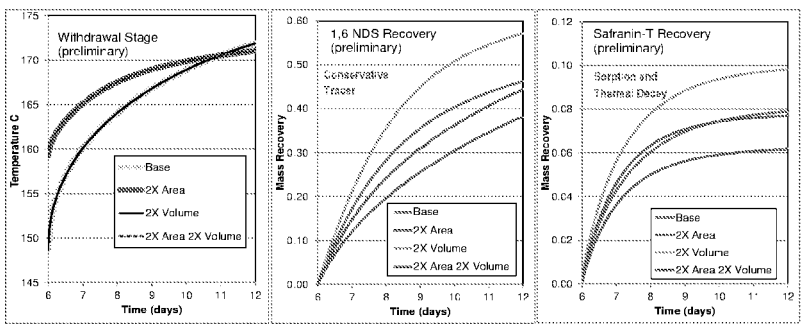

Figure 8. ToughReact simulation results showing impacts of changes in fracture surface area and fracture volume on the withdrawal stream temperatures and cumulative tracer mass recovery for the two different tracers. The withdrawal period follows (see Q1 plots) a 3 day injection period (constant concentration) and a 3 day shut-in period.

Paul Reimus, LANL:

Modeling sensitivity studies using the MULTRAN code were initiated to evaluate breakthrough curves that might be expected in both single-well and cross-hole tracer tests from quantum dot

tracers of different sizes and with different adsorption/desorption properties (relative to breakthrough curves of more conventional conservative solute tracers). The objective of this exercise is to evaluate optimal quantum dot tracer properties for interrogating various geothermal reservoir characteristics, or alternatively, to determine what reservoir characteristics can be best evaluated for a given set of quantum dot tracer properties.

Second Quarter, 2013

Paul Reimus, LANL

Shown below are simulations of experiments of the solute tracer, 1,5-naphthalene disulfonate, and the 2.6-nm yellowish quantum dots (CdSe/CdS/citrate) flowing through a sand-packed column at 25°C. The semi-analytical code RELAP captures reasonably well the behavior of both the solute and colloidal tracers.

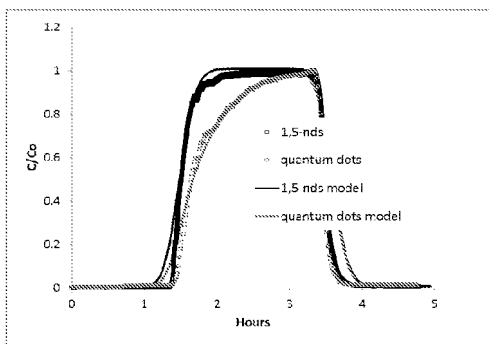

Figure 9. A plot of the measured and simulated data of the quantum dot tracer and the solute tracer flowing through a sand-packed column at 25°C.

Fourth Quarter, 2013

Task complete.

Phase 3, Subtask 3.6: <u>Synthesize sufficient quantities of sorbing quantum dot tracer(s) for field testing.</u>

Approach

At this point, only very small quantities of nonsorbing quantum dot tracers will have been synthesized for the above described testing—quantities that are insufficient for any field

demonstrations of tracer properties. For the quantum-dot tracers that have been shown to be sufficiently robust, a method will be developed to synthesize decagram quantities for testing in an EGS wellbore or reservoir. For three visibly fluorescing and one IR-fluorescing quantum dot tracer, 100 g of each will be synthesized.

First Quarter, 2013

We made significant progress in tuning synthesis parameters, resulting in an increase in yield-per-synthesis-run by a factor of about 1000. We also investigated routes to scale up our quantum dot synthesis method from the current 50-milliliter-per-synthesis run (lab scale) to liter scale and, eventually, to hundreds-of-liter scale for field testing. We demonstrated a 10-fold increase in synthesis volume without loss of the high quality and stability of quantum dots.